AECL EACL

CA9600791

Overview of Current RFSP-Code Capabilities for CANDU Core Analysis

CA9600791

AECL-11407

1996 January Janvier 1996

AECL EACL

Overview of Current RFSP-Code Capabilities for CANDU Core Analysis

AECL-11407

by B. Rouben

1996 January

Janvier 1996

2251 Speakman Drive
Mississauga, Ontario
Canada L5K 1B2

2251, rue Speakman
Mississauga (Ontario)
Canada L5K 1B2

962004/450 rouben 96/01/15

962004/450 rouben 96/01/15

AECL EACL

Overview of Current RFSP-Code Capabilities for CANDU Core Analysis

AECL-11407

by B. Rouben

Abstract

Paper presented at the 1995 Annual General Meeting of the American Nuclear Society, Philadelphia, Pa., U.S.A., 1995 June 25-29.

RFSP (Reactor Fuelling Simulation Program) is the major finite-reactor computer code in use at Atomic Energy of Canada Limited for the design and analysis of CANDU reactor cores. An overview is given of the major computational capabilities available in RFSP.

1996 January

Janvier 1996

2251 Speakman Drive
Mississauga, Ontario
Canada L5K 1B2

2251, rue Speakman
Mississauga (Ontario)
Canada L5K 1B2

62004/450
ouben
6/01/25

AECL EACL

Aperçu des possibilités de calcul actuelles du code RFSP pour l'analyse des coeurs CANDU

AECL-11407

par B. Rouben

Résumé

Le code RFSP (Reactor Fuelling Simulation Program – un programme de simulation du renouvellement du combustible) est le principal code de calcul coeur fini utilisé à Énergie atomique du Canada limitée pour la conception et l'analyse des réacteurs CANDU. On donne un aperçu des principales possibilités de calcul du code RFSP.

1996 January

2251 Speakman Drive
Mississauga, Ontario
Canada L5K 1B2

Janvier 1996

2251, rue Speakman
Mississauga (Ontario)
Canada L5K 1B2

)62004/450
'ouben
)6/01/31

TABLE OF CONTENTS

ILLUSTRATIONS

TABLE OF CONTENTS

SECTION **PAGE**

1. INTRODUCTION

RFSP (Reactor Fuelling Simulation Program) is the major computer program in use at Atomic Energy of Canada Limited for the design and analysis of CANDU reactor cores. It has seen continuing development in response to growing needs.

The major calculation method in RFSP is the solution by finite difference of the neutron-diffusion equation in three dimensions and two energy groups. However, a flux-mapping method for reconstructing the core flux distribution is also available.

The most important code capabilities will be described.

Some of the methods described herein (in particular flux mapping) are also used in the code HQSIMEX[1], employed by Hydro-Québec for the analysis of the Gentilly-2 CANDU 6 reactor.

2. TIME-AVERAGE-CORE NEUTRONICS

CANDU reactors are refuelled at power. In the CANDU 6 for example, two of the 380 fuel channels are refuelled on the average per Full Power Day (FPD). In this case an 8-bundle-shift refuelling scheme is used, where eight of the twelve fuel bundles in the channel are pushed out one end of the channel and are replaced by eight fresh bundles entering from the other end. However, the refuelling scheme need not be limited to an 8-bundle shift; 4- and 10-bundle shifts have been used, and 2-bundle shifts can be envisaged if fuels providing more reactivity than natural uranium (e.g. SEU) are used. In fact, the refuelling scheme can vary from one core region to another, or can even be specific to a particular channel. This illustrates the versatility of CANDU.

The semi-continuous refuelling in CANDU results in a global flux shape which does not vary to a great degree. One can think in terms of a time-average flux distribution about which a "refuelling ripple" is superimposed due to the burnup "journey" each channel traverses between its successive refuellings.

The time-average model is calculated within the *TIME-AVER module of RFSP. Time-average nuclear cross sections are defined at each bundle position in core by averaging the lattice cross sections over the irradiation range $[w_{in}, w_{out}]$ "experienced" over time by fuel at that position. For example, the time-average thermal neutron absorption cross section at some core position r, $\Sigma_{a2}^{t.a.}(r)$, is written as

$$\Sigma_{a2}^{t.a.}(r) = \frac{1}{(\omega_{out} - \omega_{in})} \int_{\omega_{in}}^{\omega_{out}} \Sigma_{a2}(\omega)\ d\omega \qquad (2.1)$$

where ω_{in} and ω_{out} are respectively the values of fuel irradiation when the fuel enters and exits that position in core. These will be evaluated below.

Note that the basic lattice cross sections which enter into the above integral are determined as functions of irradiation using the cell code POWDERPUFS-V[2], developed at AECL for heavy-water, natural-fuel lattices. It is incorporated in its entirety within RFSP as the *POWDERPUF module.

Let ϕ_{jk} be the time-average fuel flux at axial position k in channel j, k ranging from 1 to 12 (since there are 12 bundles per channel) and j ranging over the channels, e.g. from 1 to 380 in the CANDU 6.

Let also T_j be the average time interval between refuellings of channel j (also known as the *dwell time* of channel j).

Then the irradiation increment which the fuel at position jk will experience over its residence time at that position will be

$$\Delta\omega_{jk} = \phi_{jk}.T_j \qquad (2.2)$$

If the fuel entered position jk with an irradiation $\omega_{in,jk}$, then it will exit that position with an irradiation $\omega_{out,jk}$ given by

$$\omega_{out,jk} = \omega_{in,jk} + \Delta\omega_{jk}$$
$$= \omega_{in,jk} + \phi_{jk}.T_j \qquad (2.3)$$

When a channel is refuelled with an 8-bundle shift, the first eight positions in the channel receive fresh fuel and the entrance irradiations for positions 9-12 are simply the exit irradiations from positions 1-4 respectively. Thus we can write in this case (see Figure 2.1):

$$\omega_{in,jk} = 0 \qquad k=1,...,8 \tag{2.4a}$$

$$\omega_{in,jk} = \omega_{out,j(k-8)} \qquad k=9,...,12 \tag{2.4b}$$

For an N-bundle-shift refuelling scheme these equations become

$$\omega_{in,jk} = 0 \qquad k=1,...,N \tag{2.5a}$$

$$\omega_{in,jk} = \omega_{out,j(k-N)} \qquad k=(N+1),...,12 \tag{2.5b}$$

In addition to the refuelling scheme, we have other degrees of freedom in the time-average model. These are the values of exit irradiation $\omega_{exit,j}$ for the various channels j. In principle there are as many degrees of freedom as there are channels. (Of course the values of exit irradiation are not totally free, but are constrained by the requirement to obtain a critical reactor.) The *relative* values of $\omega_{exit,j}$ can be used to "shape" the flux to a desired reference distribution. The exit irradiations are related to the flux in the following way, written here explicitly for the 8-bundle-shift case. By definition of exit irradiation

$$\omega_{exit,j} = \frac{1}{8}\sum_{k=5}^{12} \omega_{out,jk} \tag{2.6}$$

In view of Equation (2.2) this can be written

$$\omega_{exit,j} = \frac{1}{8}\sum_{k=5}^{12} \left(\omega_{in,jk} + \phi_{jk}\ T_j\right) = \frac{1}{8}\left[\sum_{k=5}^{8} \left(\omega_{in,jk} + \phi_{jk}T_j\right) + \sum_{k=9}^{12}\left(\omega_{in,jk} + \phi_{jk}T_j\right)\right] \tag{2.7}$$

and in view of Equation (2.4) we can write

$$\omega_{exit,j} = \frac{1}{8}\left[\sum_{k=5}^{8} \phi_{jk}T_j + \sum_{k=1}^{4} \phi_{jk}T_j + \sum_{k=9}^{12} \phi_{jk}T_j\right] = \frac{T_j}{8}\sum_{k=1}^{12} \phi_{jk} \tag{2.8}$$

It is easy to derive the generalization of this result to an N-bundle-shift refuelling scheme:

$$\omega_{exit,j} = \frac{T_j}{N}\sum_{k=1}^{12} \phi_{jk} \tag{2.9}$$

The dwell time T_j must therefore satisfy

$$T_j = \frac{N\omega_{exit,j}}{\sum_{k=1}^{12} \phi_{jk}} \tag{2.10}$$

We now have all the equations required for the time-average flux distribution to be calculated. These equations are:

- the finite-difference form of the neutron diffusion equation to solve for the flux distribution,

- Equation (2.10) to compute the dwell time for each channel,
- Equation (2.5) to calculate $\omega_{in,jk}$ and $\omega_{out,jk}$ for each bundle in core,
- Equation (2.1) (and similar equations for the other cross sections) to calculate the time-average lattice properties.

This set of equations must be solved using as input the user-specified target exit irradiations $\omega_{exit,j}$. Since consistency must be achieved between the flux, the channel dwell times, the individual-bundle irradiation ranges $[\omega_{in},\omega_{out}]$, and the lattice properties, an iterative scheme between the solution of the diffusion equation and the other equations is employed until all quantities converge. (*Note: In order to ensure a reactor multiplication constant of unity, the* target exit irradiations may need to be refined and the process repeated.)

Data provided by R. Sancton and E. Young of New Brunswick Power illustrate how the CANDU 6 at Point Lepreau performed in the long run against the time-average reference core. Figure 2.2 shows statistics of the channel exit burnup (as calculated with RFSP during the tracking of the actual reactor operating history) for a database of 1865 channel refuellings in the period 1990-1992.

Note that since refuelling operations are decided day-to-day by the station physicist based on the instantaneous core state (3-d power and in-core-burnup distributions, control-rod positions, etc.), it is not possible to refuel each channel at precisely the expected dwell-time intervals. Nonetheless, the histogram in Figure 2.2 shows that the ratio of channel-average exit burnup to the time-average value follows a fairly narrow distribution, which peaks at 1.0 and falls off quickly below 0.95 and above 1.05.

As for the flux shape, Figure 2.3 compares the 1994 long-term average flux by quadrant (defined as per Figure 2.4) against the time-average flux. The deviation from time-average values is seen to be less than 1%. Figure 2.5 shows a similar comparison, but in terms of azimuthal flux profiles (defined as per Figure 2.6).

These results confirm that the time-average model closely represents the long-term average core picture.

3. INSTANTANEOUS DIFFUSION CALCULATIONS

At CANDU sites, the main application of RFSP is in tracking the reactor's operating history. This is the function of the *SIMULATE module.

Instantaneous snapshots can be calculated with diffusion theory at any desired core burnup interval. Steps of 2-3 FPD are typically convenient for the site physicist. Account is taken of the actual channel refuellings as they occur, and the core irradiation distribution is tracked together with the flux and power distributions. The effect of the spatial distribution of Xe-135 on the lattice properties (and thus on the flux distribution) is normally included in the calculation.

In the CANDU 6 reactors, there are 102 in-core vanadium detectors which are used for flux mapping. Figure 3.1 shows the location of a number of these detectors in a collapsed face view of the core. The top view of the core in Figure 3.2 shows the location of 26 vertical penetrations in which these detectors are housed.

The presence of these detectors allows the validation of the diffusion calculation against actual in-core measurements. Figures 3.3 and 3.4 illustrate the agreement typically found. They show the relative flux values from RFSP diffusion calculations at vanadium-detector positions in some regions of the Point Lepreau core, in comparison with the actual detector readings. This comparison is for a 1992 May snapshot, with the reactor at 100% FP shortly after its return to power following the annual outage.

4. RANDOM-AGE SNAPSHOTS

The *INSTANTAN module of RFSP allows the core designer to model a random day in the operating history of a reactor without resorting to a lengthy simulation of a period of operation.

The *INSTANTAN snapshots use instantaneous irradiation distributions calculated from randomly-generated channel "ages". The age A_j of channel j is a value between 0 and 1 indicating the instantaneous status of the channel in its refuelling cycle: 0 signifies that the channel has just been refuelled, 1 that it is about to be refuelled again.

The values of channel age can be chosen in the range [0,1] with a random-number generator. They are used to derive the instantaneous irradiations of all bundles in core. For a bundle at axial position k in channel j, the time-average model provides the irradiation range $[\omega_{in},\omega_{out}]$ expected to be experienced by fuel at that location. Thus, if A_j is the channel age for the snapshot being constructed, the irradiation of bundle k is

$$\omega_{jk} = \omega_{in,jk} + A_j*(\omega_{out,jk}-\omega_{in,jk}) \qquad k=1,...,12 \qquad (4.1)$$

The code can be asked to exercise some "intelligence" and avoid situations where the ages of neighbouring channels are too close to one another, i.e., where neighbouring channels have been refuelled at approximately the same time, leading to a "hot spot" in the core.

The *INSTANTAN user can also define a "patterned" random distribution of ages over a small number of channels, which is then repeated over the entire core. Figure 4.1 is an example of a 7x7 patterned random distribution.

5. HISTORY-BASED METHODOLOGY FOR LATTICE PROPERTIES

Lattice properties have in the past been calculated by interpolating in irradiation within "fuel tables" computed by the cell code, assuming core-average values of such parameters as the fuel temperature and coolant density; this is the "uniform-parameter" method.

However, lattice properties do depend on the local values of these parameters, and also on the history of quantities such as the moderator poison concentration.

Core-modelling detail has recently seen a major degree of improvement in the development of the "history-based" methodology[3], for use especially in core tracking. In this method, fuel tables are not employed. At each core-follow snapshot, an individual POWDERPUFS-V calculation is performed within RFSP for each fuel bundle to update its properties over the incremental burnup step, using *locally appropriate* values of parameters (flux level, fuel temperature, coolant density, whatever parameters the user specifies) for that instant in the core history.

Changes in lattice parameters are therefore modelled when they actually occur, and the evolution of the nuclear properties of each individual bundle is more properly tracked. The diffusion equation is then solved as usual.

The history-based method as well as the conventional method of computing core properties can be validated by comparing calculated flux distributions with in-core-detector readings[4]. Such activities can be and are in fact carried out routinely during core-follow. Figures 5.1 and 5.2 show some results, in the form of the standard deviation of differences between the 102 calculated and measured vanadium-detector readings. The figures span two extended periods (each about 150 FPD) in the operating history of the Point Lepreau reactor.

It can be seen that both methods of calculating lattice properties provide good agreement with detector readings. The history-based simulation does, however, lead to a further improvement (a reduction of about 0.2 to 0.5 in the standard deviation of percent differences) compared to the conventional (uniform-parameter) method.

Physics tests are often performed during the return to power of a reactor following an outage. Such tests provide another opportunity to validate RFSP, in particular the history-based method. In 1991 in Gentilly-2 and in 1992 in Point Lepreau a number of flux measurements were made in core with a Travelling Flux Detector (TFD). Measurements were made both for a nominal core configuration (i.e. with reactivity devices in their nominal position) and for configurations with reactivity devices moved from their nominal position, e.g. adjuster banks withdrawn from core or shutoff rods inserted in core.

New Brunswick Power commissioned a comprehensive simulation, with the history-based methodology, of the tests carried out at Point Lepreau. Figure 5.3 shows the standard deviation of differences between calculated and measured detector responses for several control-rod configurations. Figures 5.4-5.7 illustrate the excellent agreement typically attained between the calculated flux shape and the TFD flux scans (Figures 5.8-5.11 clarify the reactivity-device configurations).

6. FLUX MAPPING

RFSP has a flux-mapping capability. The readings of the in-core vanadium detectors are used to "synthesize" the 3-d flux distribution as a linear superposition of some 15 basis functions ("modes"), harmonics of the steady-state diffusion equation. The first ten harmonics are shown schematically in Figure 6.1. Flux mapping is also used in the code HQSIMEX [1], used by Hydro-Québec at the Gentilly-2 CANDU 6 reactor.

The mode amplitudes are computed by least-squares fitting the synthesized ("mapped") fluxes to the detector readings. Standard deviations of about 2% between mapped and measured detector fluxes are routinely achieved.

Some of the physics tests during the 1992 Point Lepreau startup were also simulated with flux mapping, using the detector readings recorded at the time of the tests. A compilation of all the simulation results by H. Chow [5] shows that the flux-mapping method in fact gave the best agreement to TFD flux scans and vanadium-detector readings for a whole range of nominal and perturbed core configurations (see Figure 5.3).

Flux mapping has the advantage that it uses data from within the reactor core to compute the instantaneous core picture. Hydro-Québec was the first utility to take advantage of this characteristic by adopting flux mapping as the standard tool for core follow at Gentilly-2 [1a]. New Brunswick Power has followed suit by adopting it at Point Lepreau in the last few years.

7. SPATIAL KINETICS

RFSP has, in its *CERBERUS module, a spatial-kinetics capability, which can be used to analyze fast transients. The most typical application of this is in the evaluation of the power pulse which may result from a hypothetical loss-of-coolant accident (LOCA), and of the shutdown-system performance in terminating the excursion.

In the *CERBERUS module, the time-dependent neutron diffusion equation with delayed-neutron terms is solved using the Improved Quasi-Static method [6]. Here the flux is written as the product of an amplitude depending on time only and a space-and-time-dependent shape function.

Separate (but coupled) equations are developed for the shape function, the amplitude, and the delayed-neutron precursors. The factorization allows the frequency of the (computationally onerous) shape calculation to be greatly reduced: flux-shape time steps of the order of 50-100 ms can be used in LOCA calculations. These can be thought of as "macro" time steps.

The point-kinetics-like set of equations for the amplitude and core-integrated precursor concentrations requires much less computational effort and a smaller ("micro") time step can be used for this component of the problem within each "macro" time step.

The solution scheme incorporates iterations between the flux-shape and amplitude solutions at each shape time step, to ensure cross-consistency between all quantities.

This method has been validated using results of tests at the Savannah River Laboratory [7] and of shutdown-system tests in CANDU reactors [8-10]. Comparison to measurements has been consistently excellent. Figures 7.1 and 7.2, for example, show, for a Point Lepreau Shutdown System No. 1 test carried out in 1992 May, the very close agreement between the flux rundown as measured with in-core instrumentation and that calculated with RFSP.

Calculations of a LOCA require a knowledge of the change in coolant density (voiding) with time. This is determined with a thermalhydraulics calculation. Since the degree of voiding may be dependent on the initial power or power distribution, or even on the power pulse itself, the neutronics calculation in *CERBERUS has been coupled to the thermalhydraulics calculation (performed outside RFSP).

8. MODELLING OF THE REACTOR REGULATING SYSTEM

Recently, Hydro-Québec and New Brunswick Power have commissioned AECL to add to RFSP the ability to model the action of the reactor regulating system (RRS) in the CANDU 6. This capability is now incorporated in the new *CERBRRS module of RFSP, where it is coupled to the neutronics calculation (see Figure 8.1).

The *CERBRRS module allows the simulation of transients where reactivity devices are manipulated by the RRS to manoeuvre the reactor power or adjust the core power distribution. The actual algorithms used by the RRS to perform these functions have been incorporated in subroutines within RFSP.

The functionality of this new feature of RFSP has been verified and documented [11]. Figures 8.2 to 8.4 from this reference illustrate the actions of the RRS as *predicted* by RFSP in the case of an operator-requested power reduction and of a small in-core loss of coolant respectively.

Validation of *CERBRRS calculations against actual plant data is at the study and planning stage.

9. REFERENCES

1. a) G. Hotte, A. Baudouin, and G. Parent, "Gentilly Core Management Based on Diffusion Theory and On-Line Monitoring", in Proceedings of the American Nuclear Society Topical Meeting on Advances in Fuel Management, Pinehurst, N.C., U.S.A., 1987.

   b) G. Hotte, M. Beaudet, and D. Brissette, "Flux-Mapping Application Using In-Core-Detector Measurements for Fuel Management at the Gentilly-2 NGS", IAEA Meeting of the Working Group on Advanced Technologies for Water-Cooled Reactors, Toronto, Ont., Canada, 1993 June.

2. B. Rouben, "Description of the Lattice Code POWDERPUFS-V", AECL-11357, 1995 October.

3. B. Rouben and D.A. Jenkins, "A Review of the History-Based Methodology for Simulating CANDU Reactor Cores", in Proceedings of INC93 (International Nuclear Congress 93), Toronto, Ont., Canada, 1993 October, ISBN-0-919784-34-8, Session C23, Vol.3.

4. A.C. Mao, B. Rouben, D.A. Jenkins, C. Newman, and E. Young, "Validating the History-Based Methodology for Core Tracking Using In-Core Detectors", in Proceedings of INC93 (International Nuclear Congress 93), Toronto, Ont., Canada, 1993 October, ISBN-0-919784-34-8, Session C23, Vol.3.

5. H. Chow and C. Newman, "Post-Simulations of Point Lepreau 1992 Startup Physics Tests", in Proceedings of the 15th Annual Conference of the Canadian Nuclear Society (Session 3B), Montreal, Qué., Canada, 1994 June, ISSN 0227-1907.

6. K.O. Ott and D.A. Meneley, "Accuracy of the Quasistatic Treatment of Spatial Reactor Kinetics", Nucl. Sci. Eng. 36,402 (1969).

7. G. Kugler and A.R. Dastur, "Accuracy of the Improved Quasistatic Space-Time Method Checked with Experiment", AECL-5553, 1976 October.

8. B. Rouben, A.R. Dastur, G. Kugler, and H.Y.H. Li, "Confirmation of CANDU Shutdown System Design and Performance During Commissioning", in Proceedings of the American Nuclear Society Topical Meeting on Reactor Safety, Idaho Falls, Idaho, U.S.A., 1977 July.

9. R.D. McArthur et al., "Simulation of CANDU 6 (CANDU 600) LISS Tests", in Proceedings of the 16th Nuclear Simulation Symposium, Canadian Nuclear Society, Saint John, N.B., Canada, 1991 August.

10. D.A. Jenkins and E.G. Young, "Simulation of the 1992 SDS1 Trip Test at Point Lepreau", in Proceedings of the 1994 Nuclear Simulation Symposium, Canadian Nuclear Society, Pembroke, Ont., Canada, 1994 October.

11. H.C. Chow, B. Rouben, M.H. Younis, D.A. Jenkins, A. Baudouin, and P.D. Thompson, "Simulation of Reactor Regulating System Action in RFSP", in Proceedings of the 16th Annual Conference, Canadian Nuclear Society, Saskatoon, Sask., Canada, 1995 June.

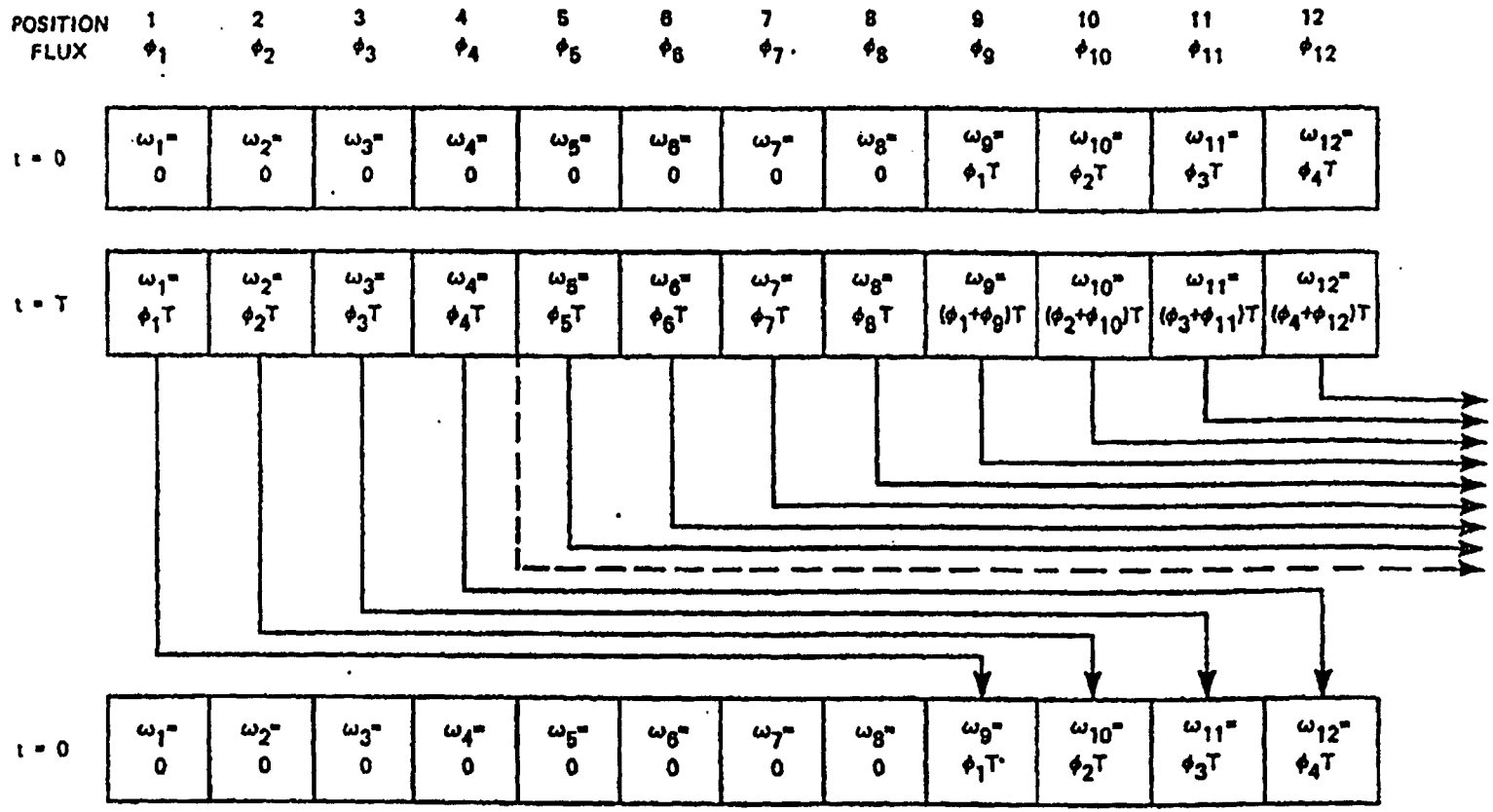

AVERAGE DISCHARGE IRRADIATION

$$= \frac{1}{8} \left\{ \phi_5 T + \phi_6 T + \phi_7 T + \phi_8 T + (\phi_1 + \phi_9)T + (\phi_2 + \phi_{10})T + (\phi_3 + \phi_{11})T + (\phi_4 + \phi_{12})T \right\}$$

$$= \frac{T}{8} \left\{ \phi_1 + \phi_2 + \phi_3 + \phi_4 + \phi_5 + \phi_6 + \phi_7 + \phi_8 + \phi_9 + \phi_{10} + \phi_{11} + \phi_{12} \right\}$$

Figure 2.1 Eight-Bundle-Shift Channel in Time-Average Model

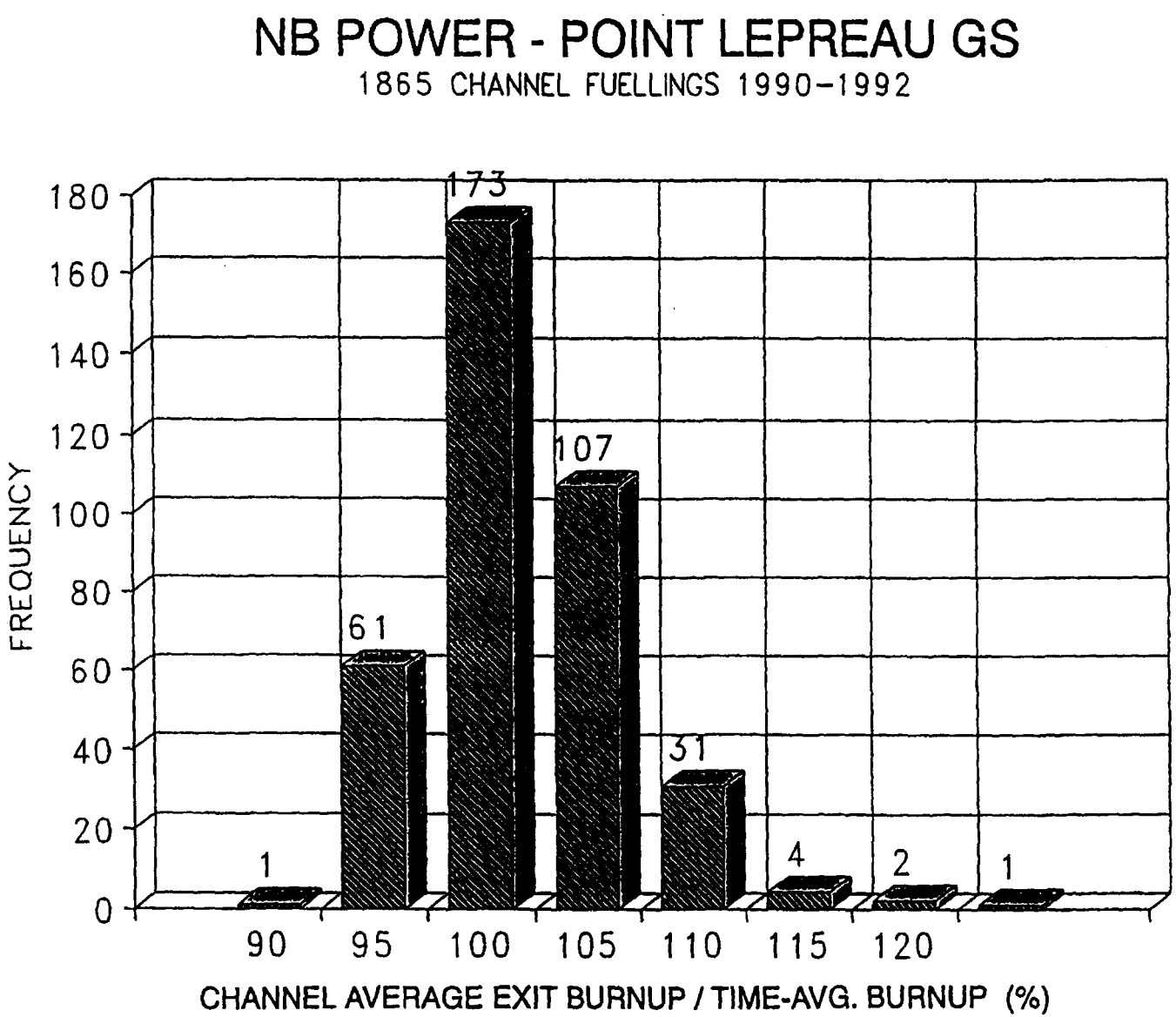

Figure 2.2 Core-Follow Exit Burnup Compared to Time-Average-Model Prediction

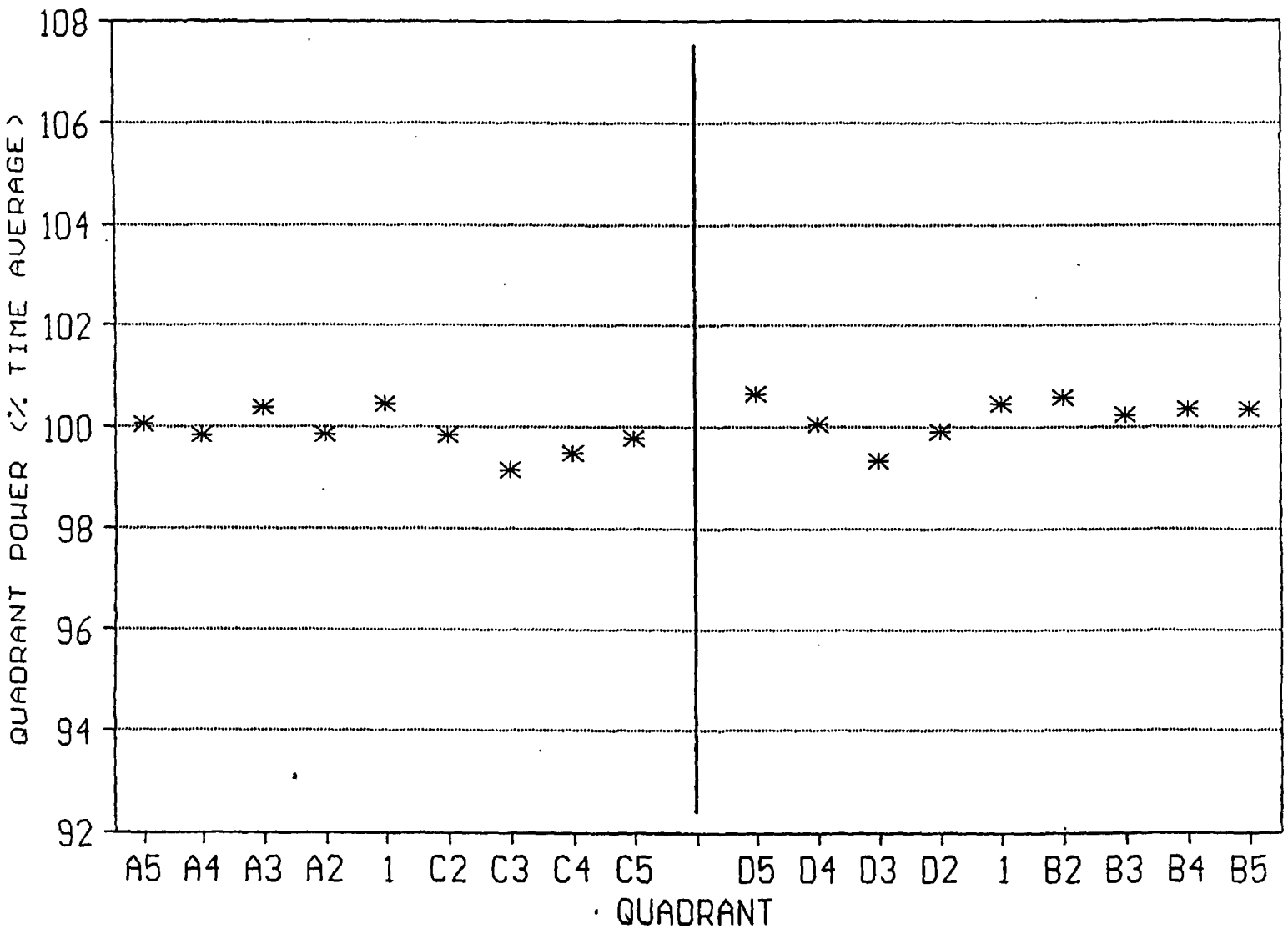

Figure 2.3 Power Profile by Quadrant (Point Lepreau, 1994)

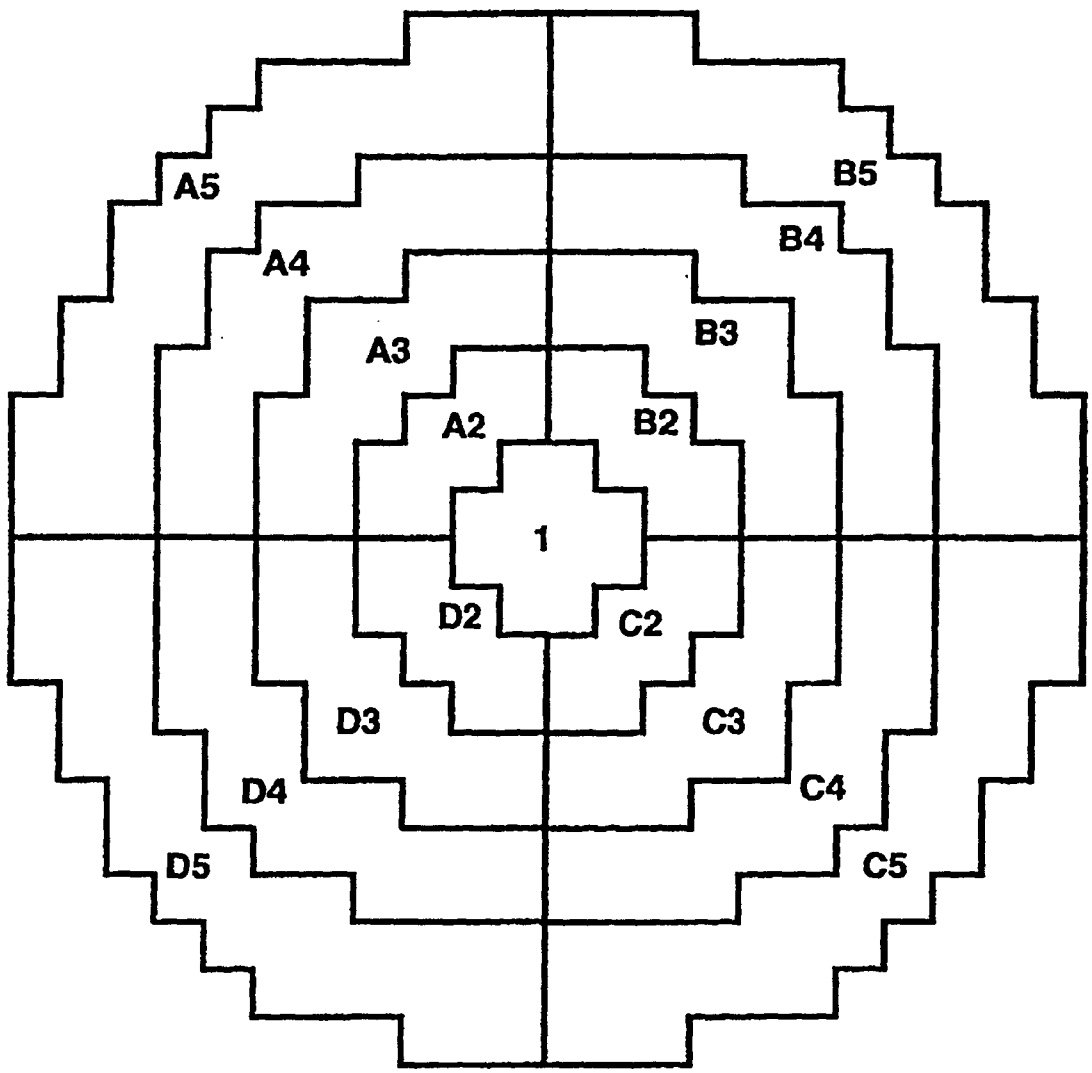

Figure 2.4 Definition of Quadrants for Figure 2.3

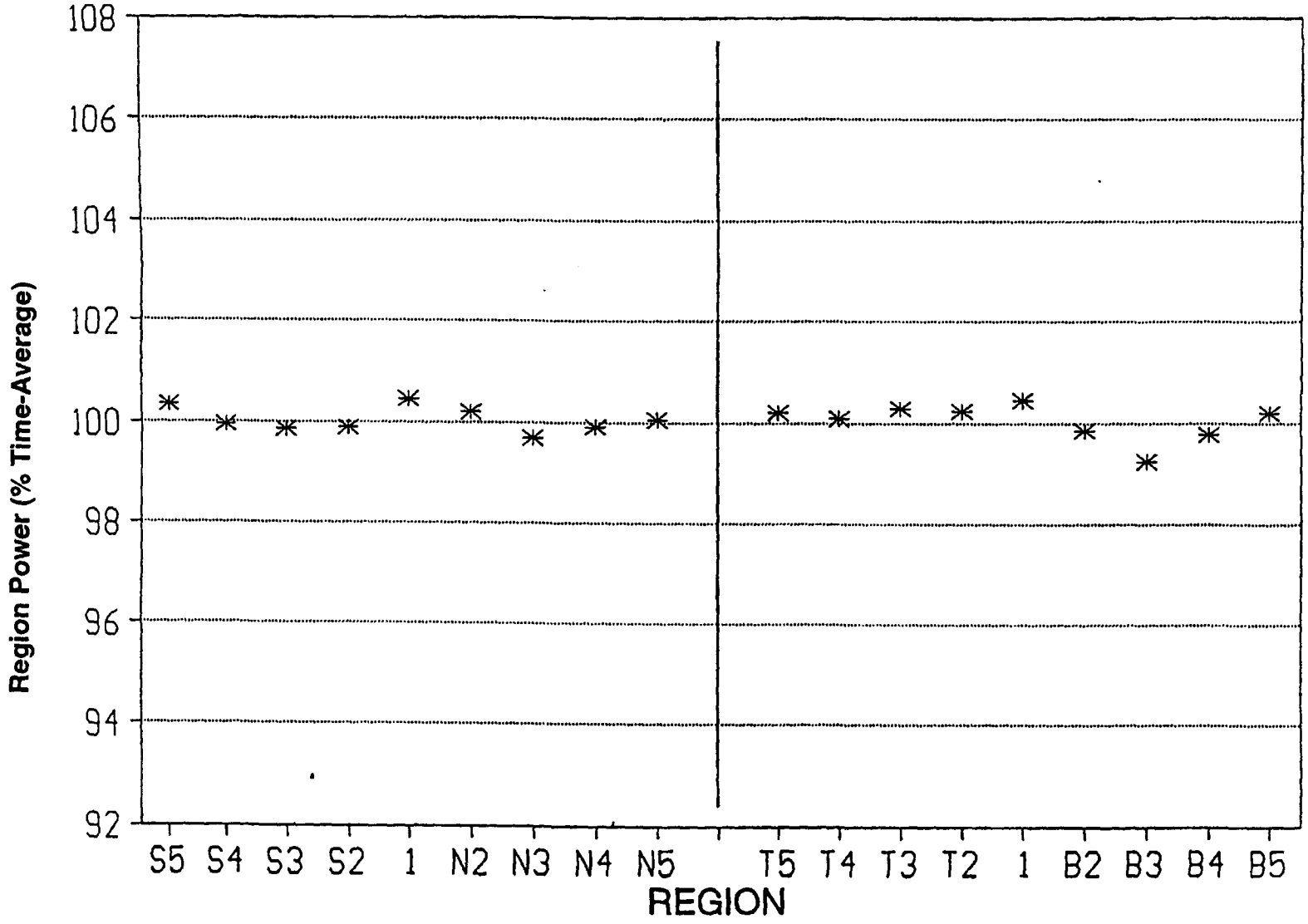

Figure 2.5 Side-to-Side and Top-to-Bottom Power Profiles (Point Lepreau, 1994)

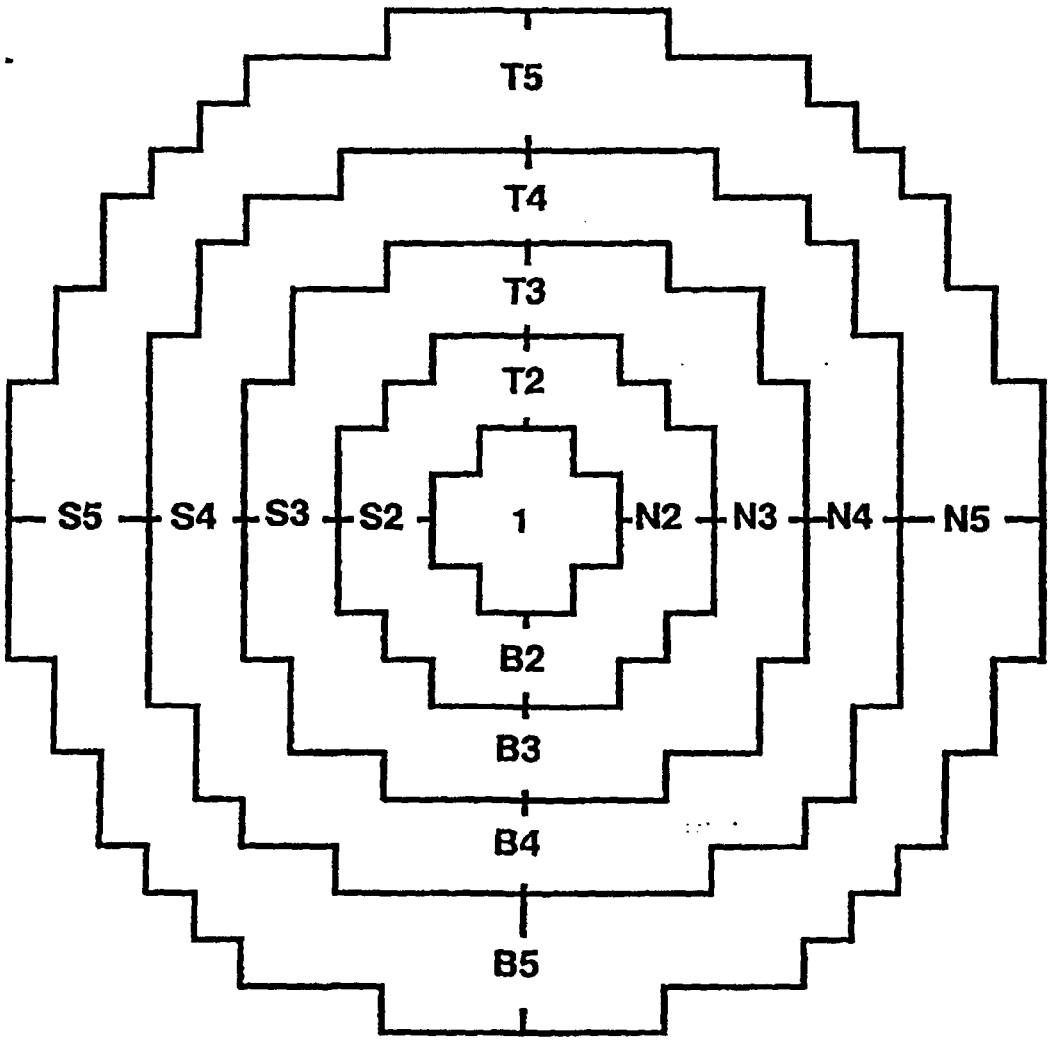

Figure 2.6 Definition of Quadrants for Figure 2.5

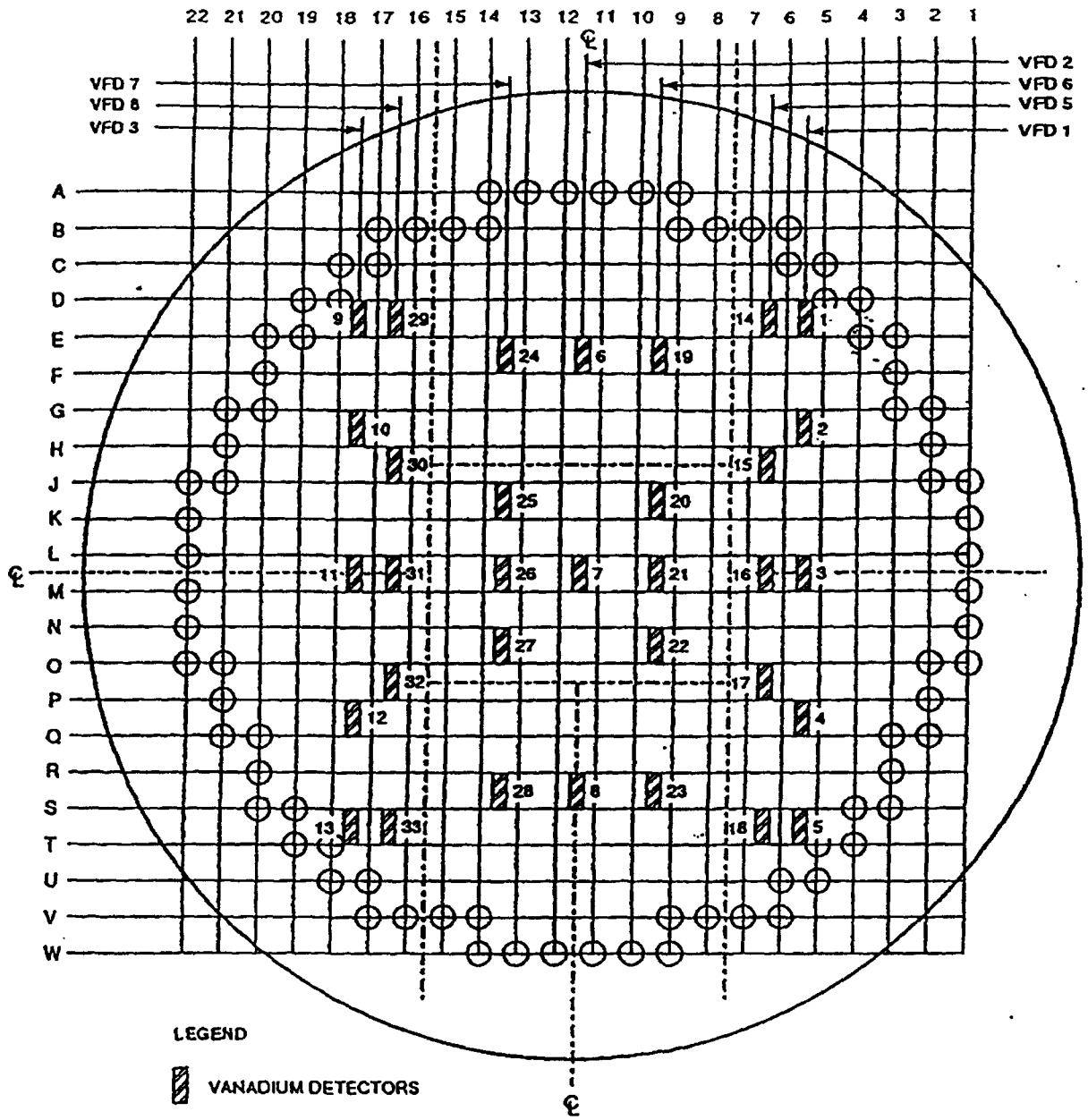

Figure 3.1 Location of Some Flux-Mapping Vanadium Detectors (Point Lepreau)

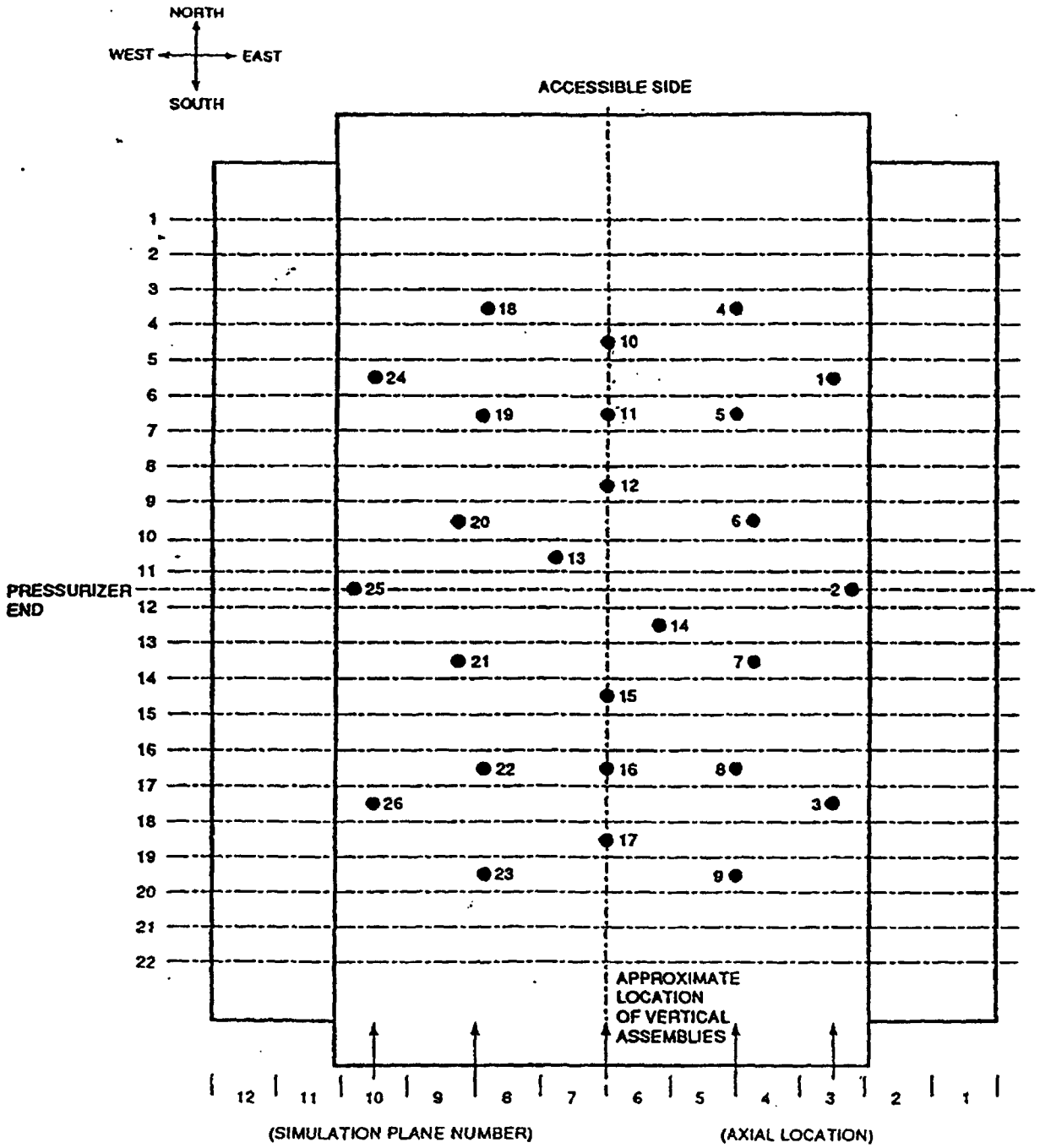

Figure 3.2 Location of Vertical Flux-Detector Assemblies in CANDU 6 (Top View)

VANADIUM FLUX COMPARISON
NOMINAL CORE AT 100% POWER

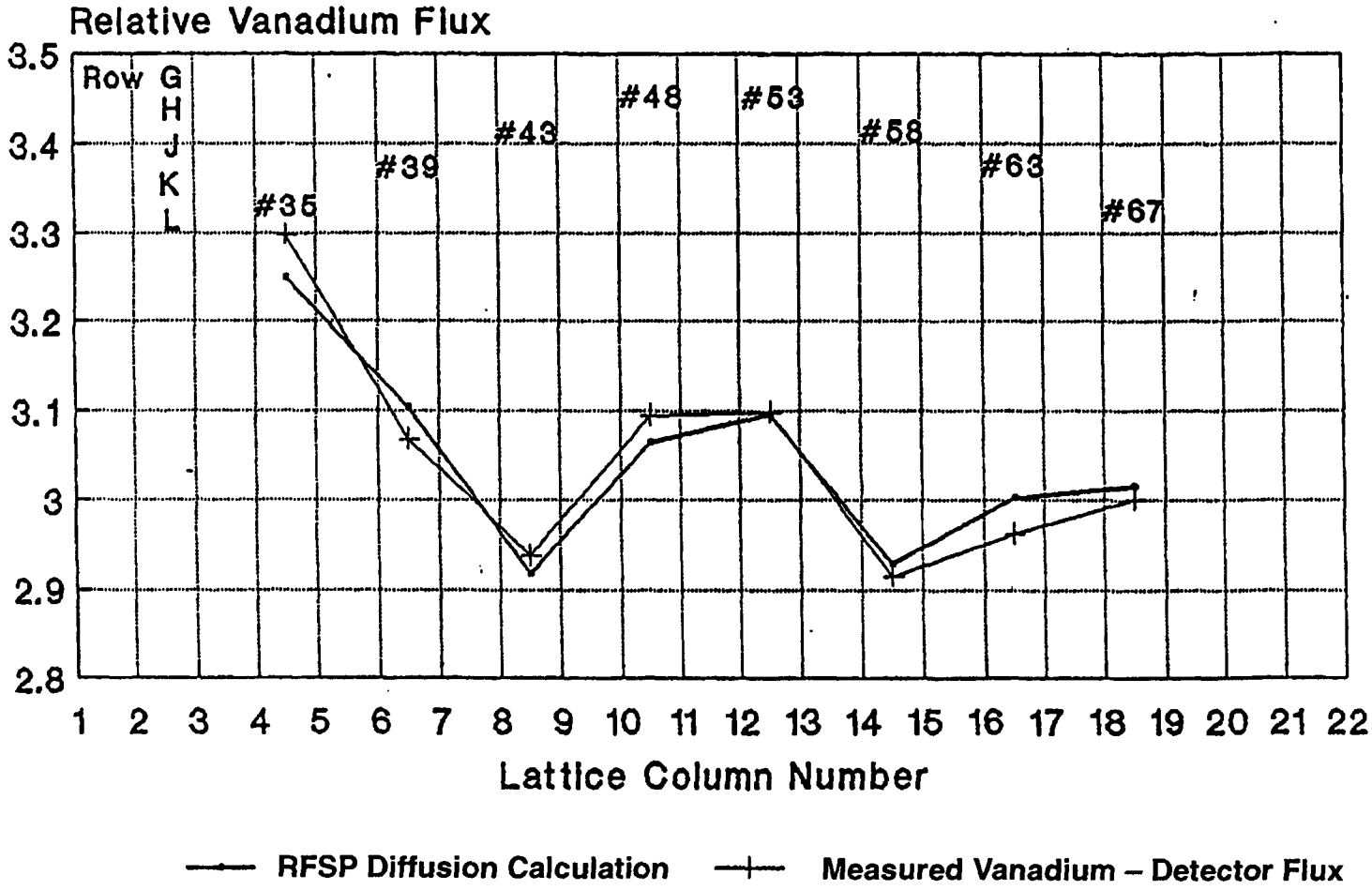

Figure 3.3 Calculated and Measured Vanadium-Detector Fluxes in Nominal Core (Set 1)

VANADIUM FLUX COMPARISON
NOMINAL CORE AT 100% POWER

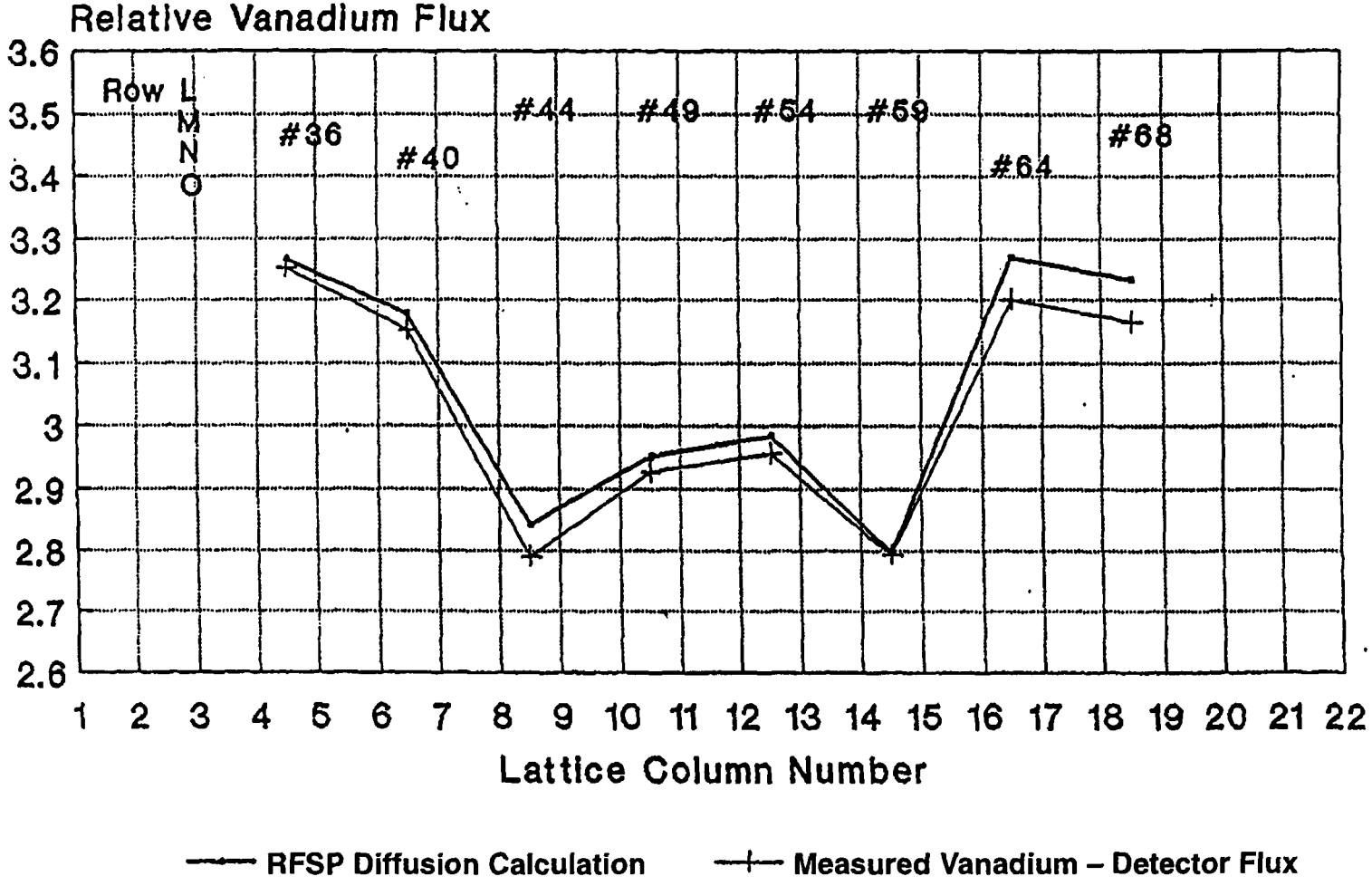

Figure 3.4 Calculated and Measured Vanadium-Detector Fluxes in Nominal Core (Set 2)

.54	.96	.02	.48	.36	.70	.16
.76	.22	.68	.26	.90	.08	.42
.30	.56	.10	.80	.52	.18	.64
.84	.38	.92	.50	.78	.32	.86
.72	.34	.60	.98	.74	.40	.62
.06	.88	.46	.24	.20	.94	.12
.44	.14	.04	.66	.58	.28	.82

Figure 4.1 Random Channel-Age Pattern (7 x 7 Region)

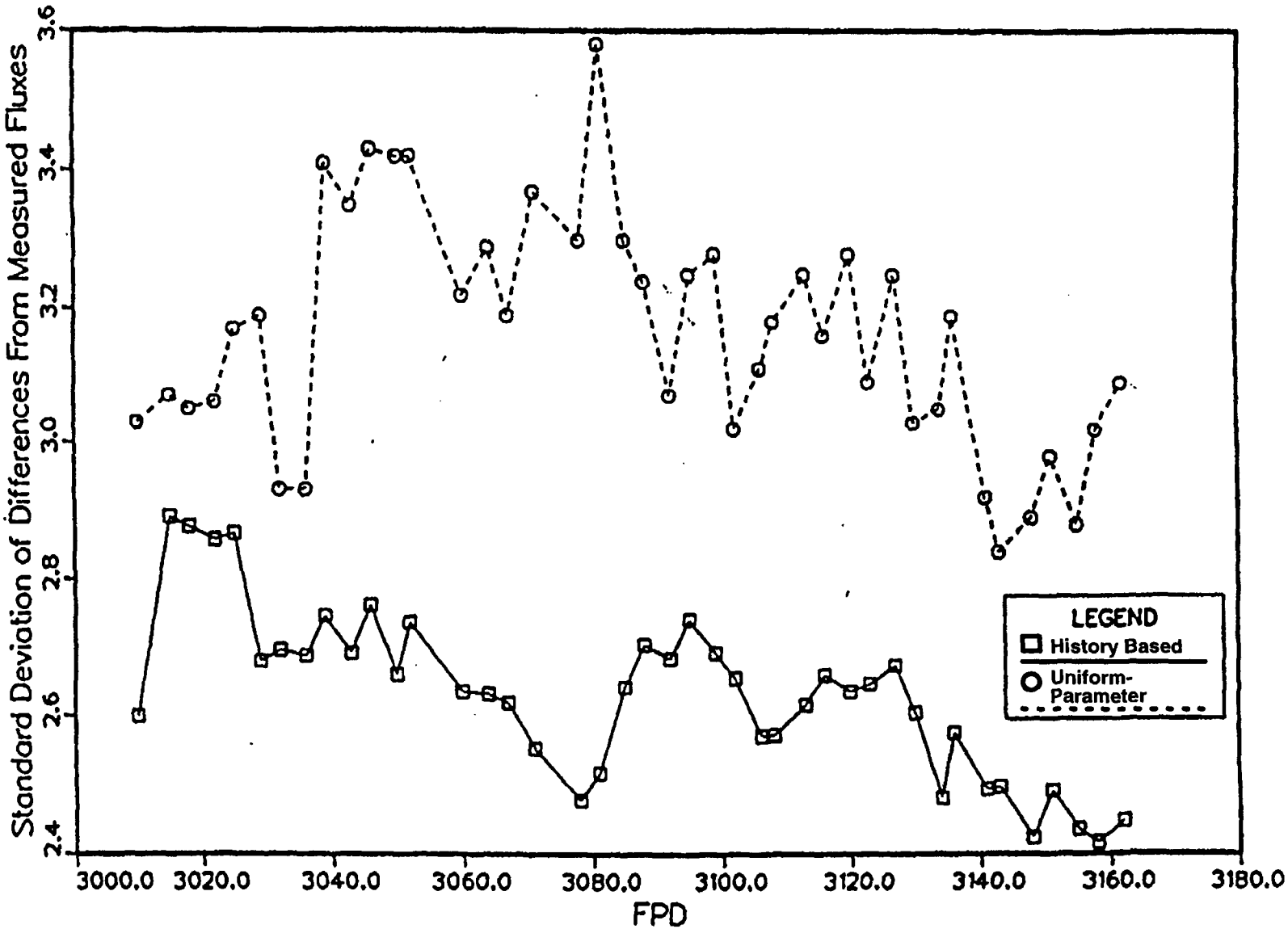

Figure 5.1 Core-Follow Simulated and Measured V-Detector Fluxes

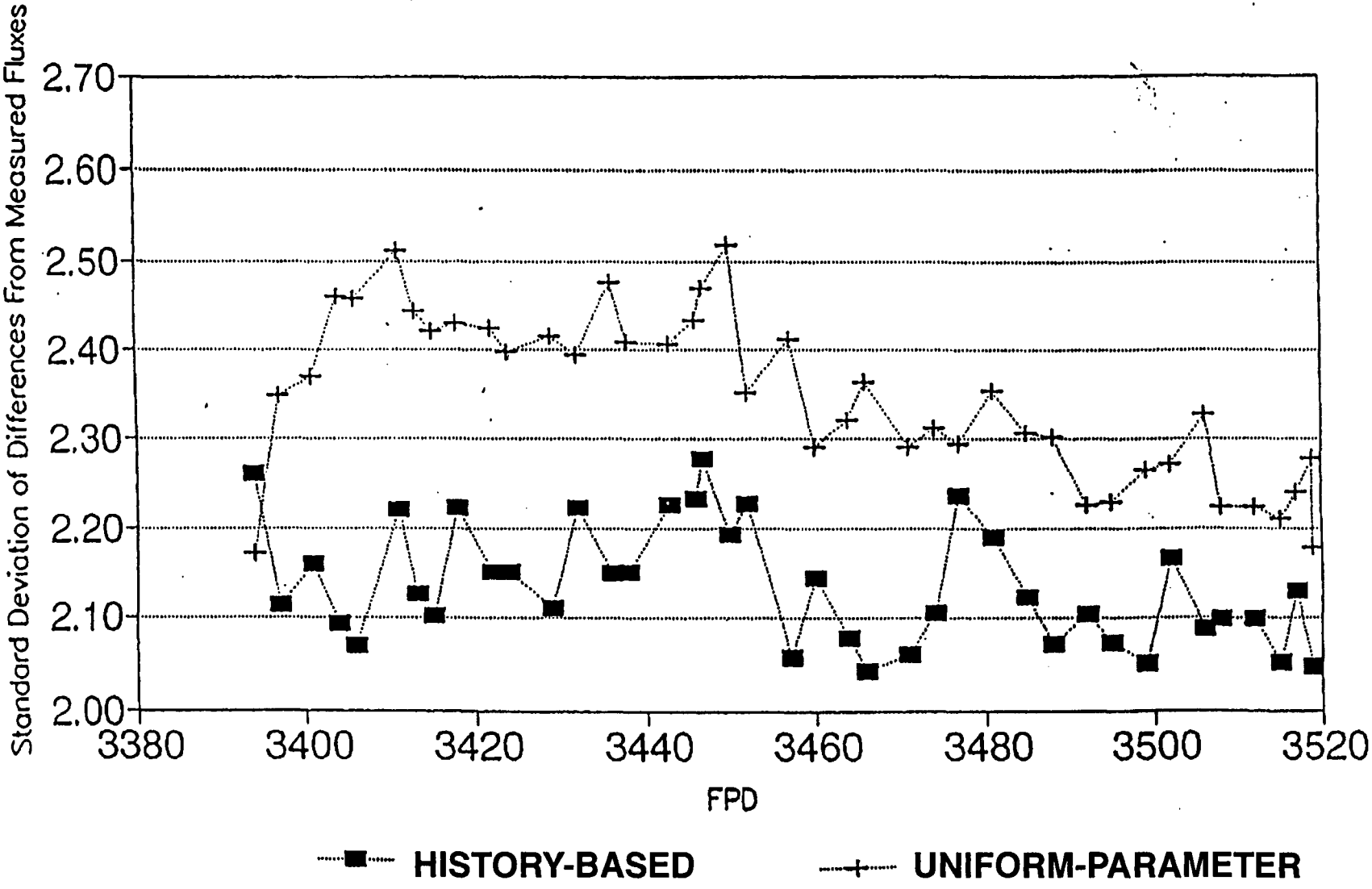

Figure 5.2 Comparison of History-Based and Conventional Core-Follow Methods

Simulation Method	Perturbation						Average
	MCA1/4 Half–In	SOR19 Half–In	Zone 2 Drain	AA 18 Out	1–Bank Shim	4–Bank Shim	
Uniform-Parameter Diffusion	1.2	1.4	2.8	2.6	2.5	1.5	2.0%
History–Based Diffusion	1.2	1.3	1.6	2.3	2.5	1.8	1.8%
Mapping	0.6	0.7	0.3	0.3	0.3	0.3	0.4%

Figure 5.3 Comparison of Perturbations in RFSP and Measured V-Detector Fluxes

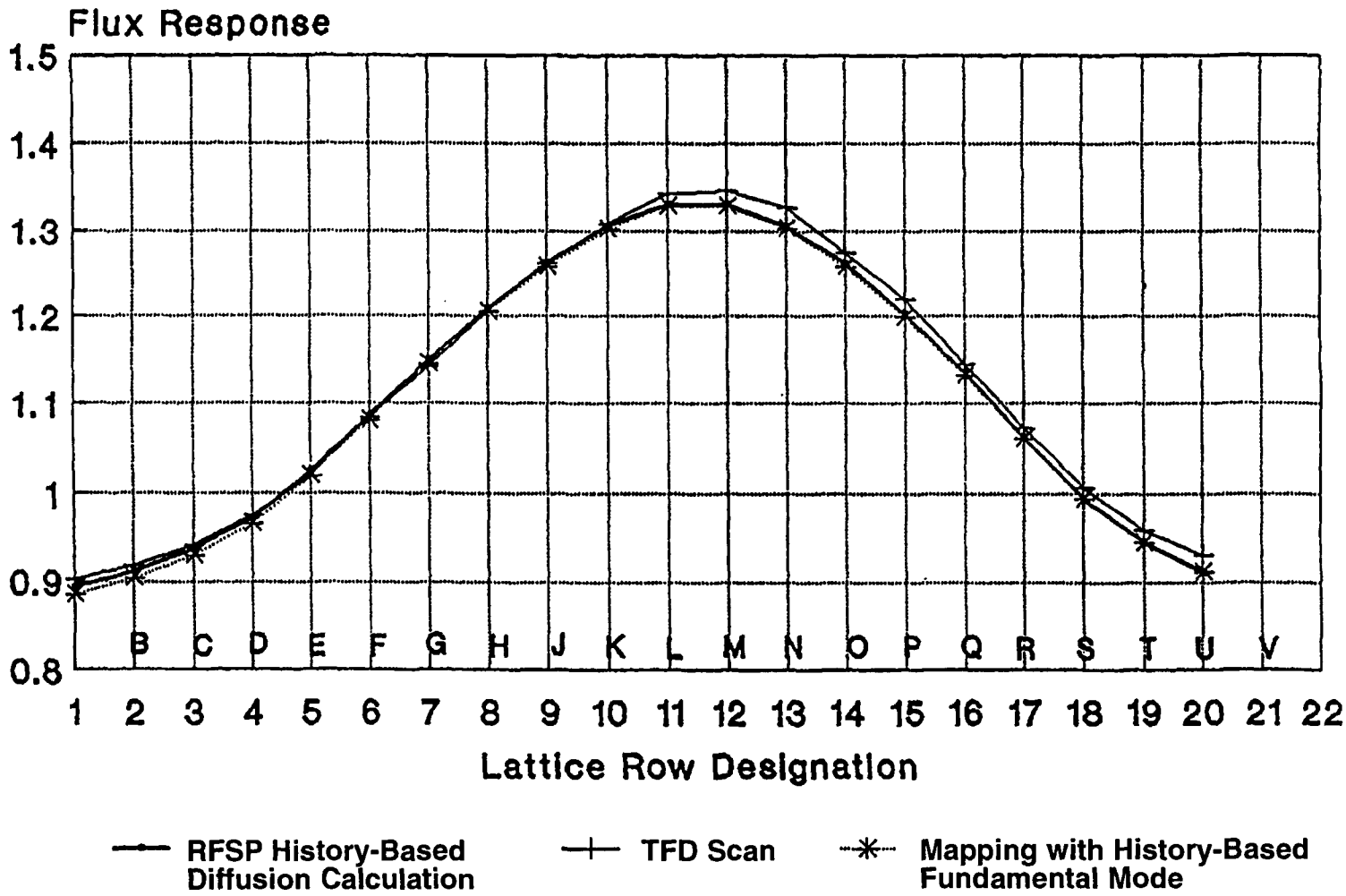

Figure 5.4 TDF Flux Scan in VFD13 (Four Adjuster Banks Out-of-Core, 50% FP)

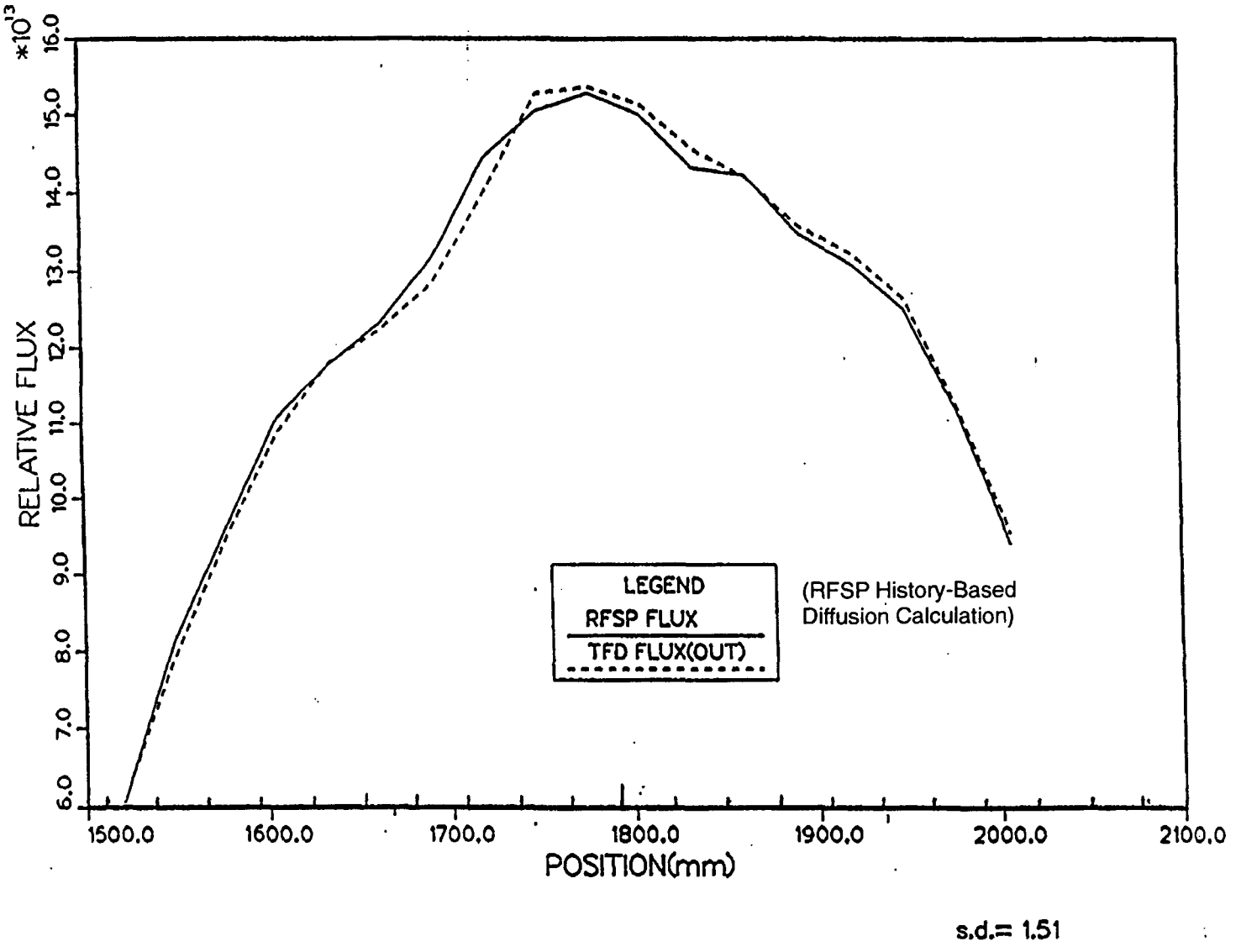

Figure 5.5 TFD Flux Scan in VFD25 (Four Adjuster Banks Out-of-Core, 50% FP)

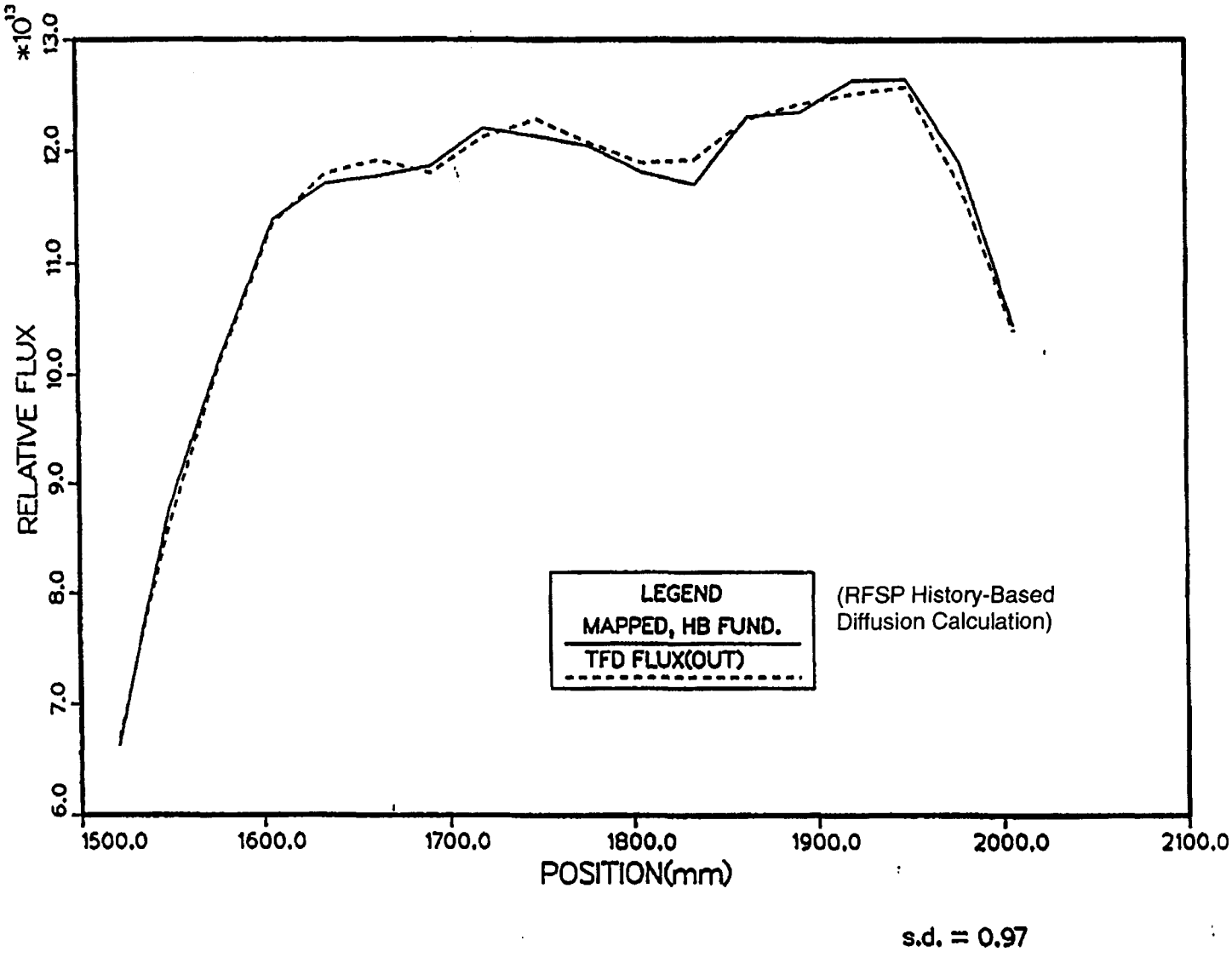

Figure 5.6 TFD Flux Scan in VFD19 (SOR 19 55% Inserted, 50% FP)

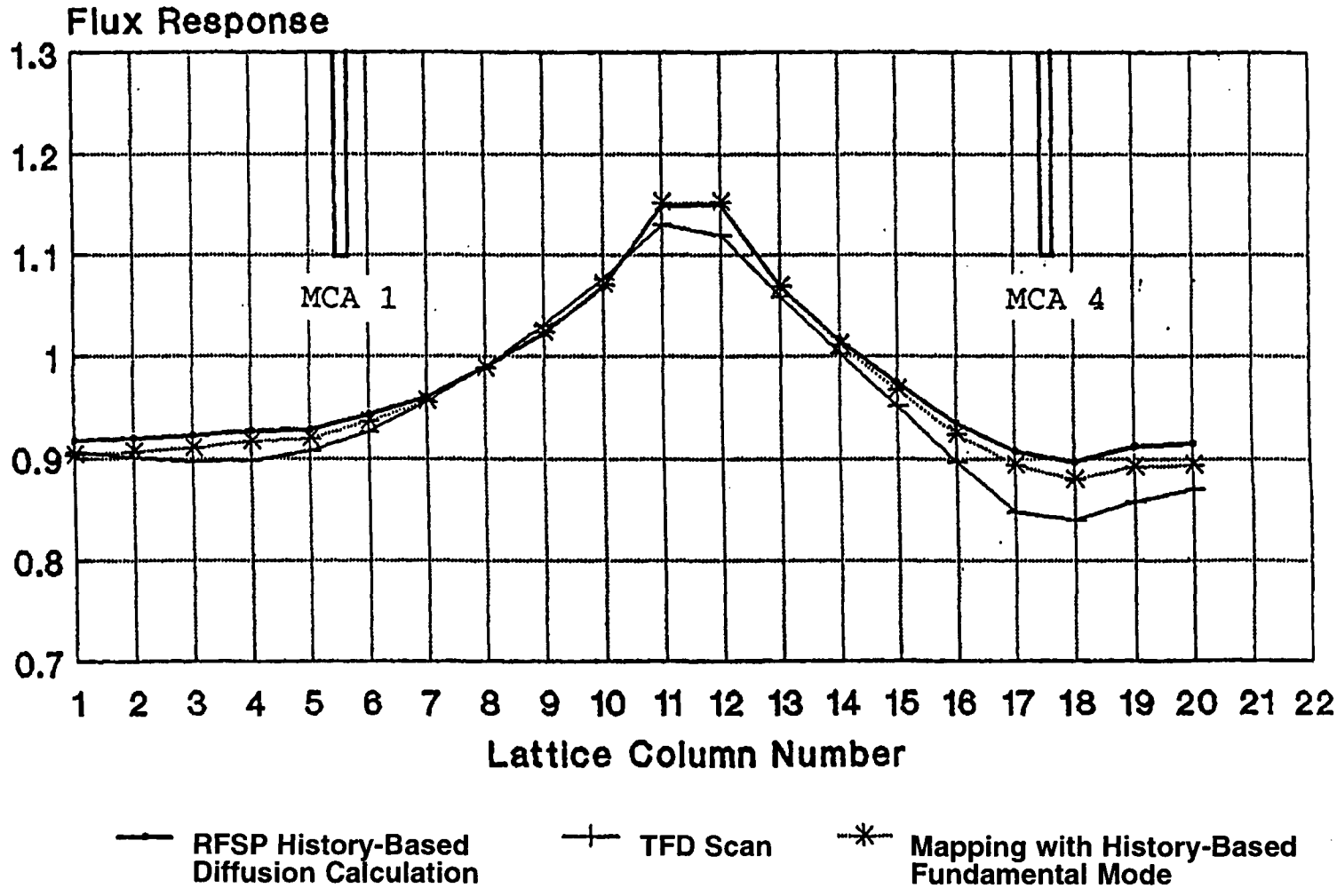

Figure 5.7 Flux Response in HD3 (MCA Bk. 1 Half In, Adjuster Bk. 1 Out, 50% FP)

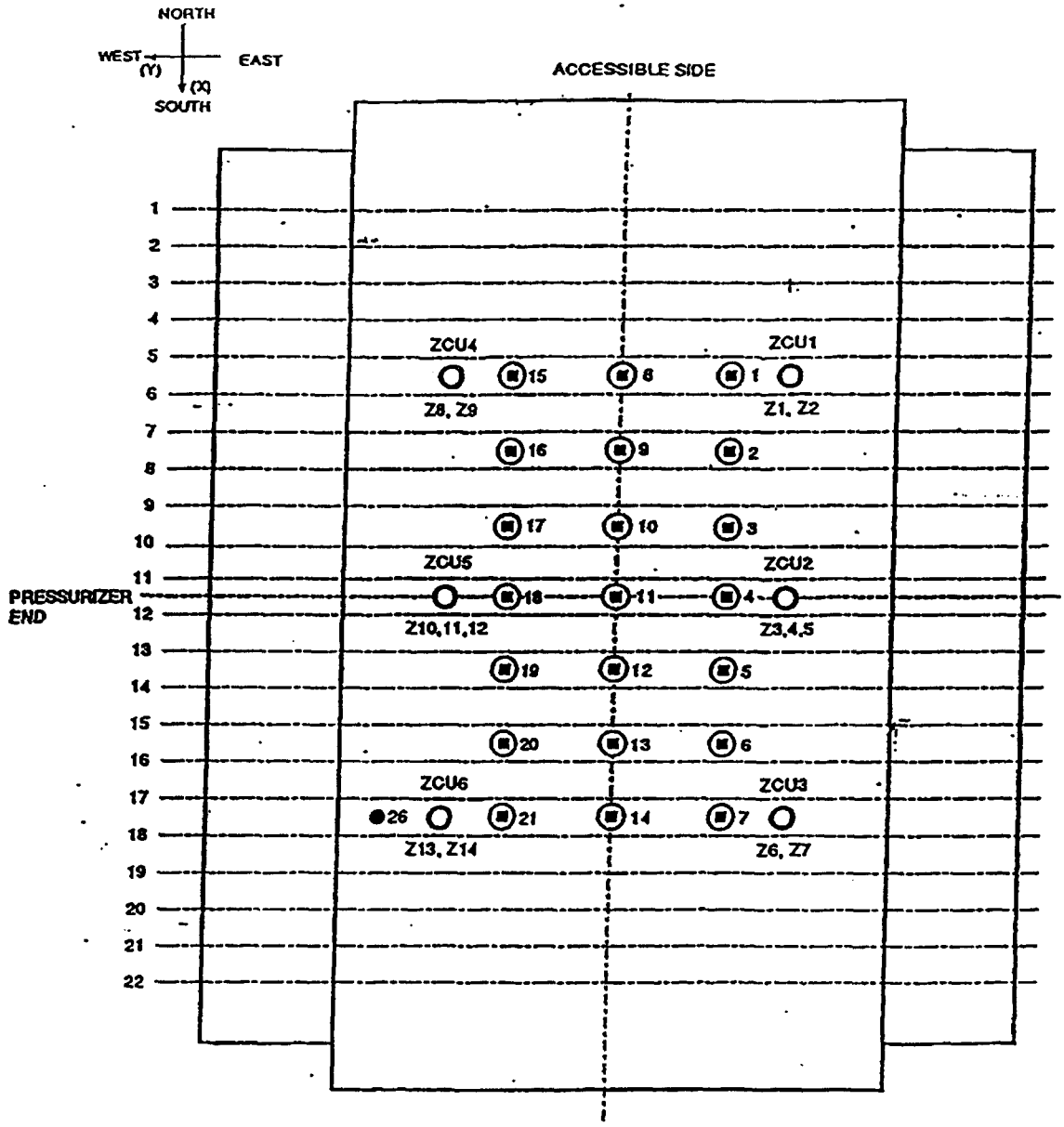

ADJUSTER BANKING	BANK NO.	ADJUSTERS
	1	1, 7, 11, 15, 21
(BANK 1 IS FIRST WITHDRAWN FOR SHIM)	2	2, 6, 18
	3	4, 16, 20
(BANK 7 IS FIRST REINSERTED DURING STARTUP)	4	8, 9, 13, 14
	5	3, 19
	6	5, 17
	7	10, 12

Figure 5.8 Adjuster Banking Scheme in CANDU 6

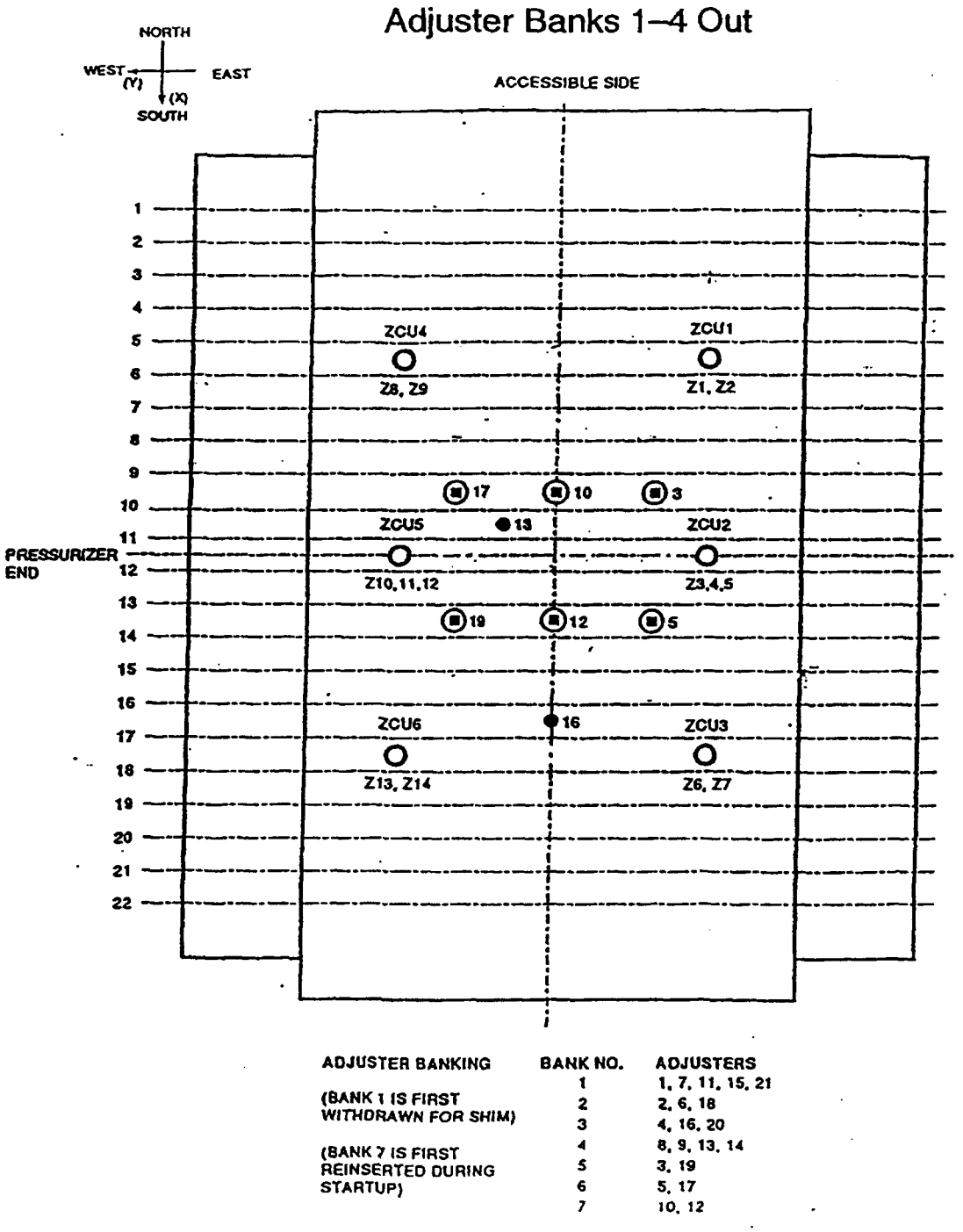

Figure 5.9 Adjuster Rods Remaining in Core when Banks 1-4 are Withdrawn

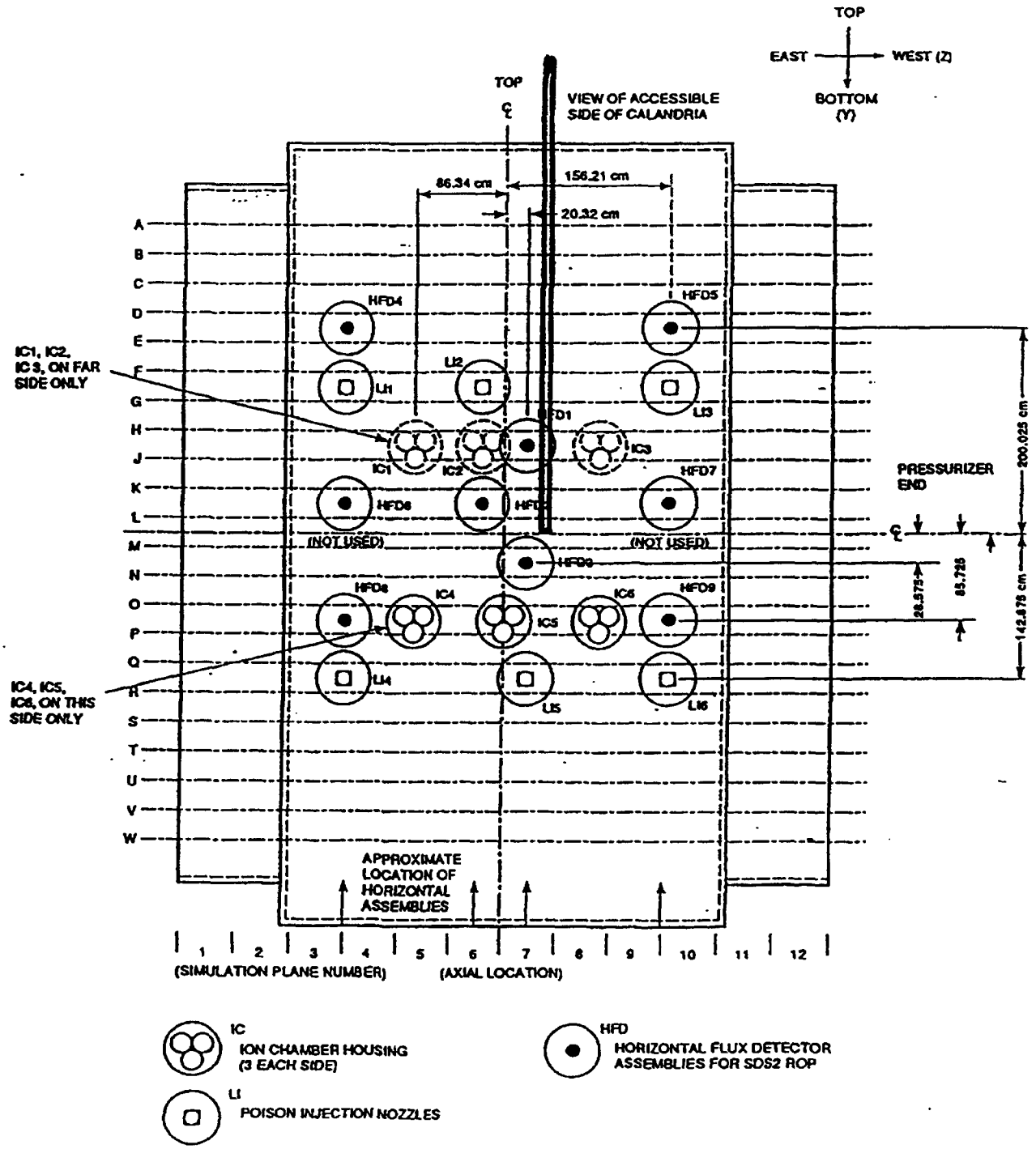

Figure 5.10 Position of SOR 19 when 55% Inserted in Core – Side View

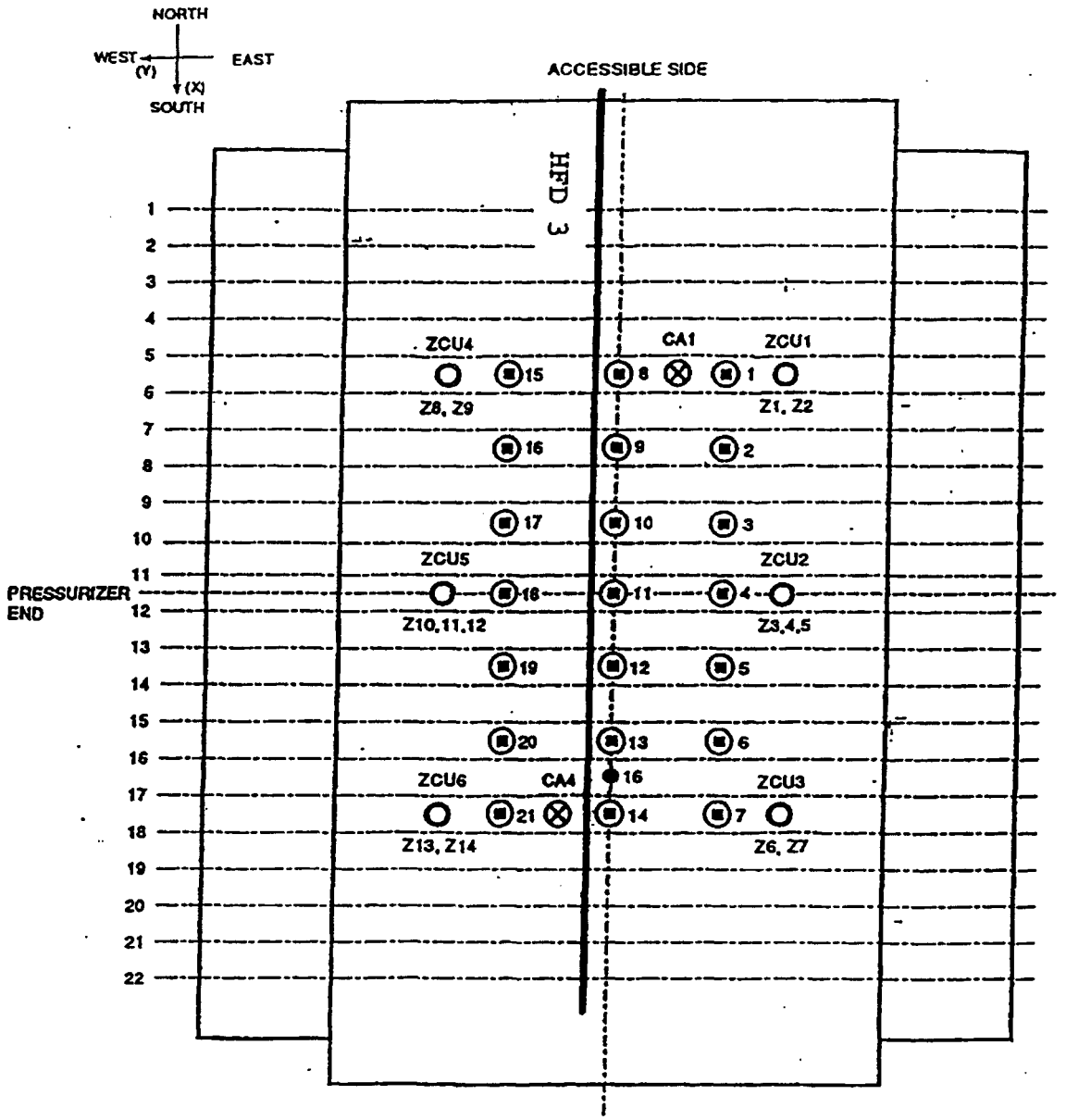

ADJUSTER BANKING	BANK NO.	ADJUSTERS
(BANK 1 IS FIRST WITHDRAWN FOR SHIM)	1	1, 7, 11, 15, 21
	2	2, 6, 18
	3	4, 16, 20
(BANK 7 IS FIRST REINSERTED DURING STARTUP)	4	8, 9, 13, 14
	5	3, 19
	6	5, 17
	7	10, 12

Figure 5.11 Location of Horizontal Flux-Detector Assembly HFD 3 (Top View)

MODE NUMBER	DESIGNATION	SUBCRITICALITY mk	MODE SCHEMATIC (IDEALIZED)
0	FUNDAMENTAL	0	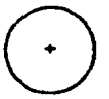
1	FIRST AZIMUTHAL-A	16.2	
2	FIRST AZIMUTHAL-B	16.9	
3	FIRST AXIAL	27.1	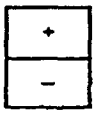
4	SECOND AZIMUTHAL-A	44.0	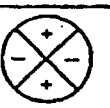
5	SECOND AZIMUTHAL-B	47.0	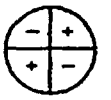
6	FIRST AZIMUTHAL-A X FIRST AXIAL	46.9	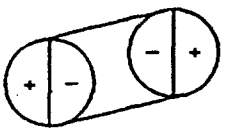
7	FIRST AZIMUTHAL-B X FIRST AXIAL	47.7	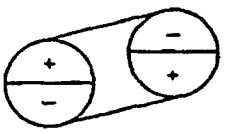
8	FIRST RADIAL X SECOND AXIAL-A	66.3	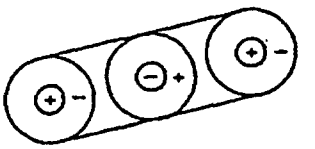
9	FIRST RADIAL X SECOND AXIAL-B	80.6	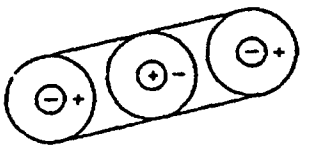

Figure 6.1 Flux Harmonics Used in CANDU 6 Flux Mapping

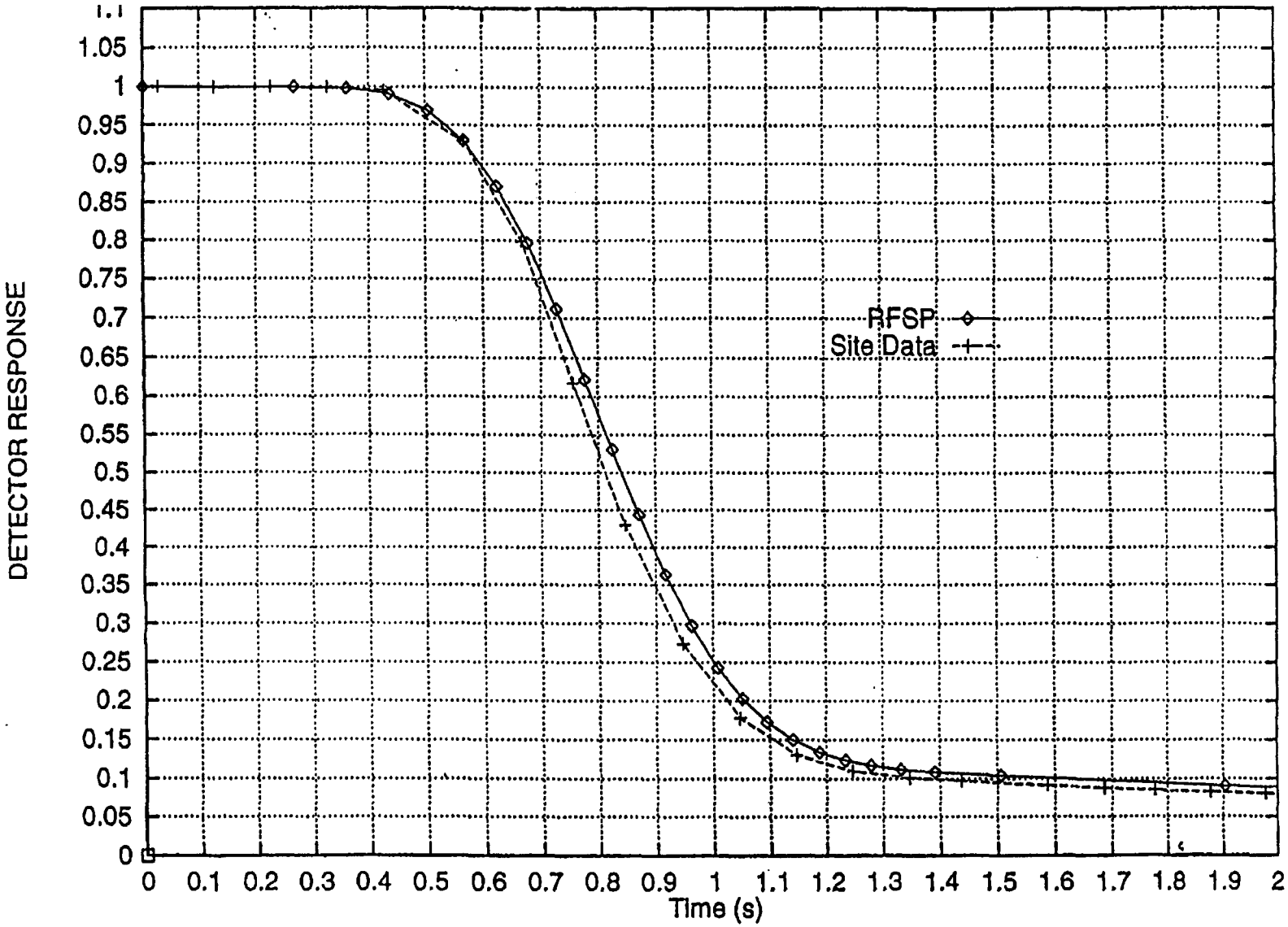

Figure 7.1 Response of ROP Detector 4F in 1992 SDS1 Trip Test at Point Lepreau

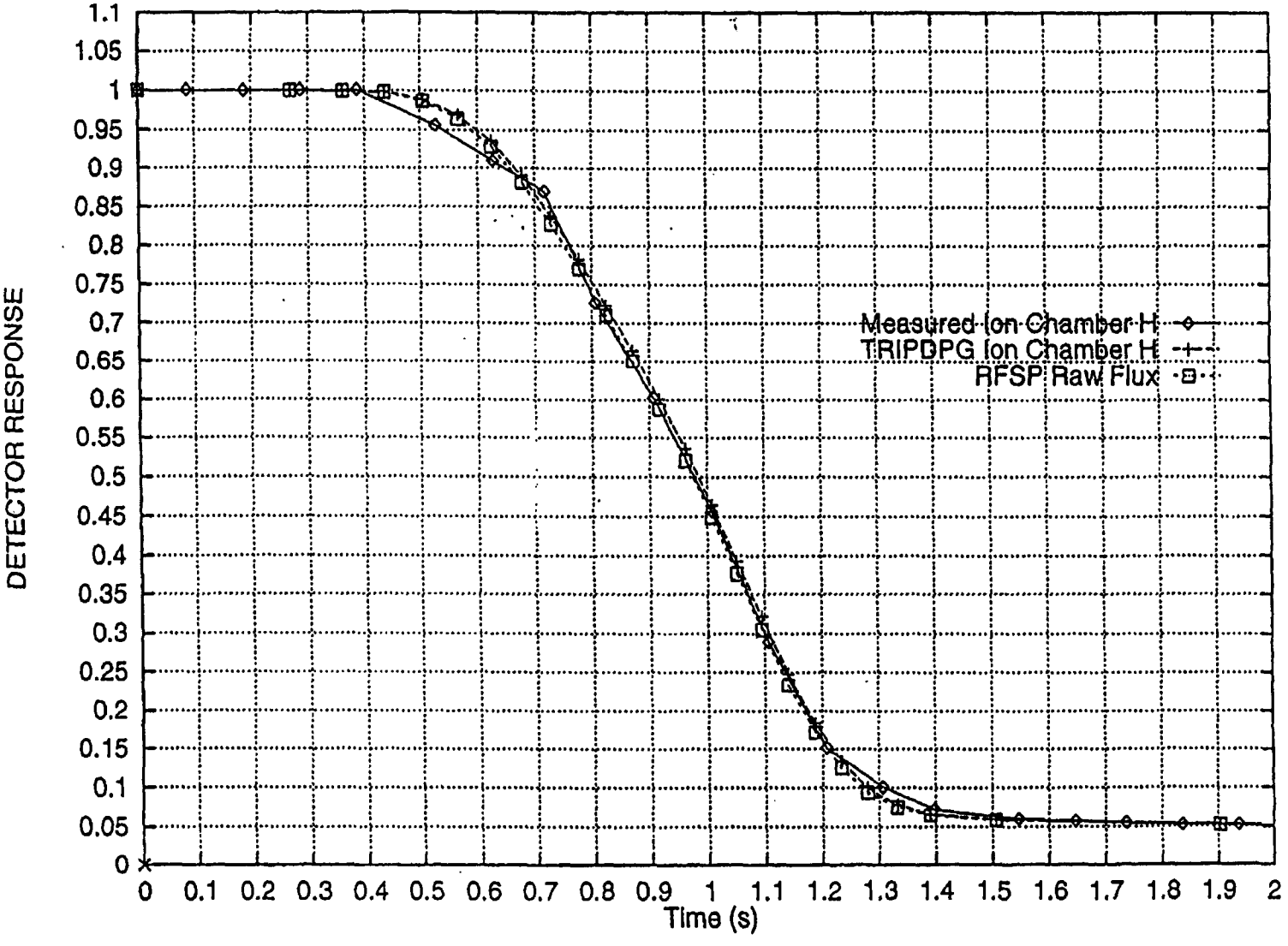

Figure 7.2 Response of Ion Chamber H in 1992 SDS1 Trip Test at Point Lepreau

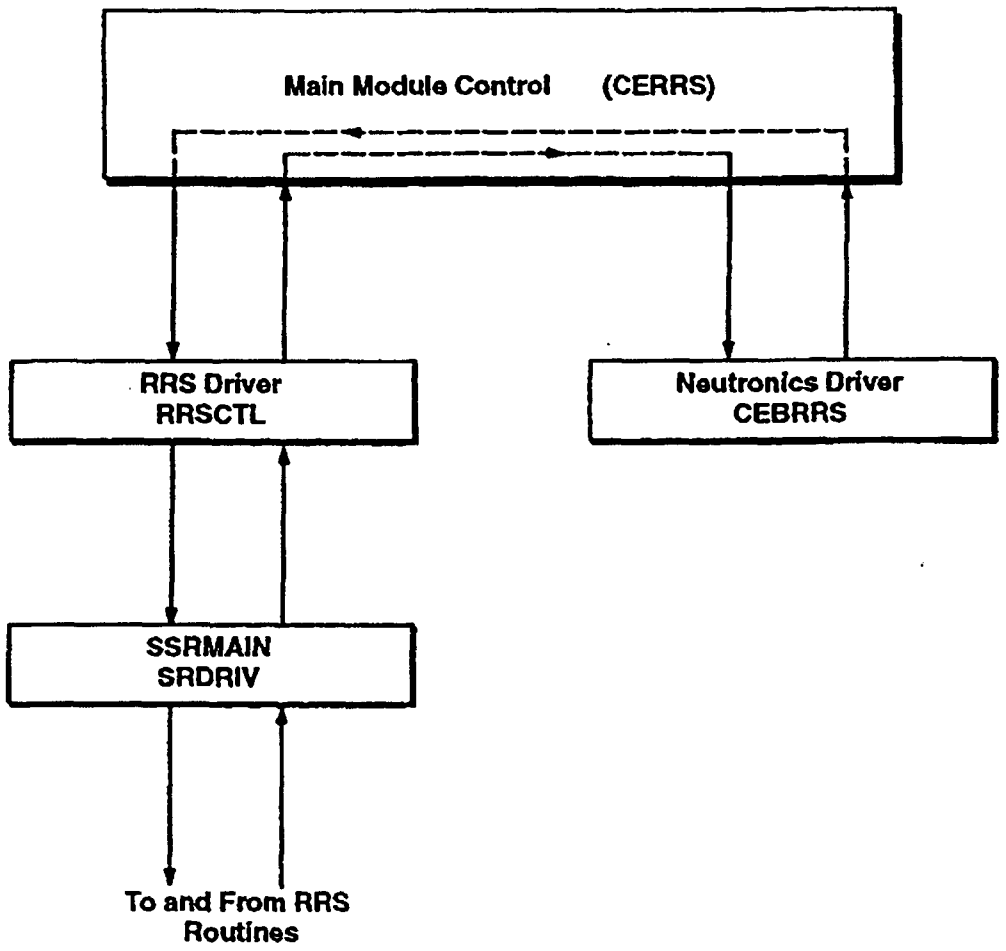

Figure 8.1 Flow Chart of *CERBRRS Module

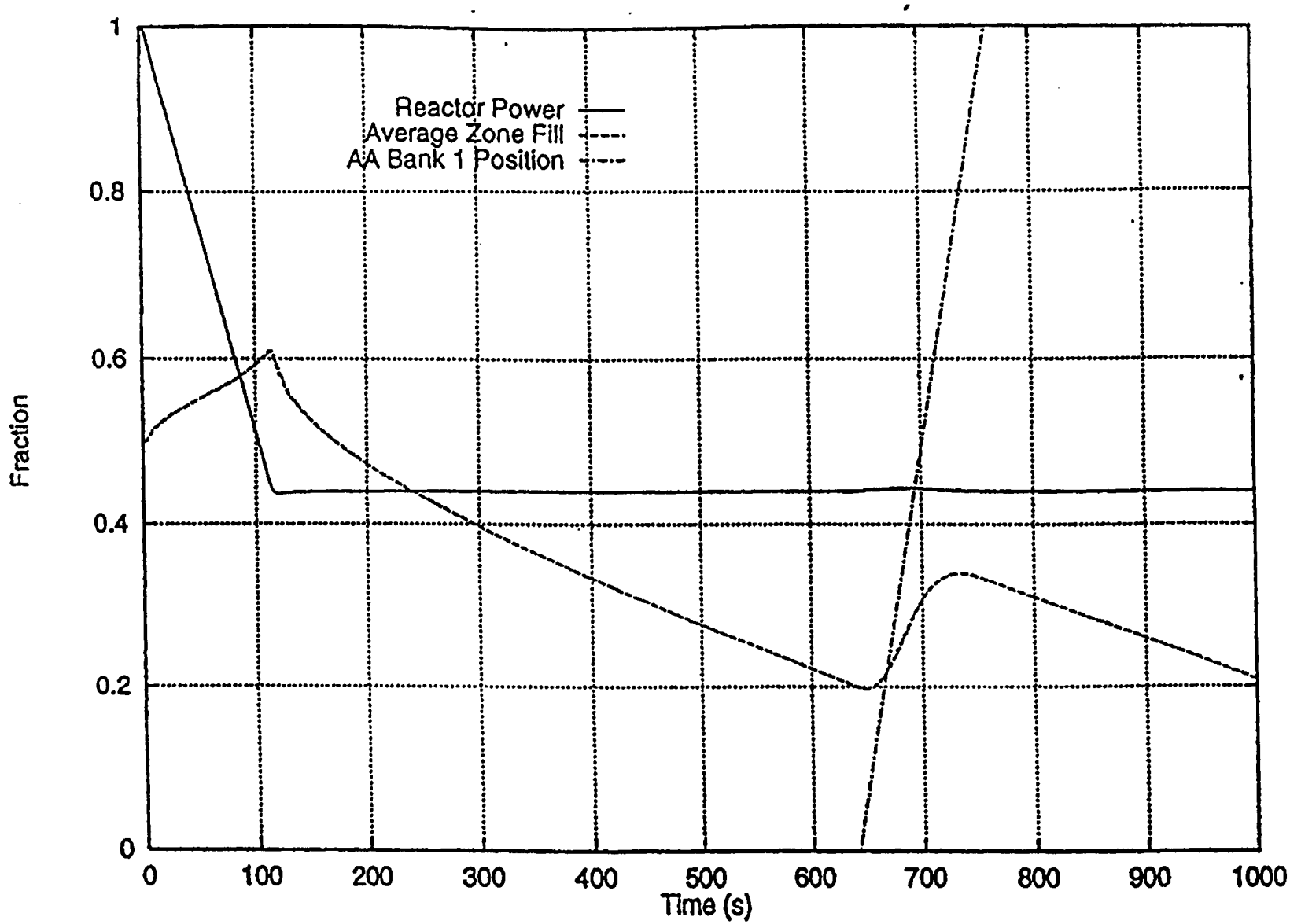

Figure 8.2 Power-Reduction Test – 100% to 44% FP (CERBRRS Results)

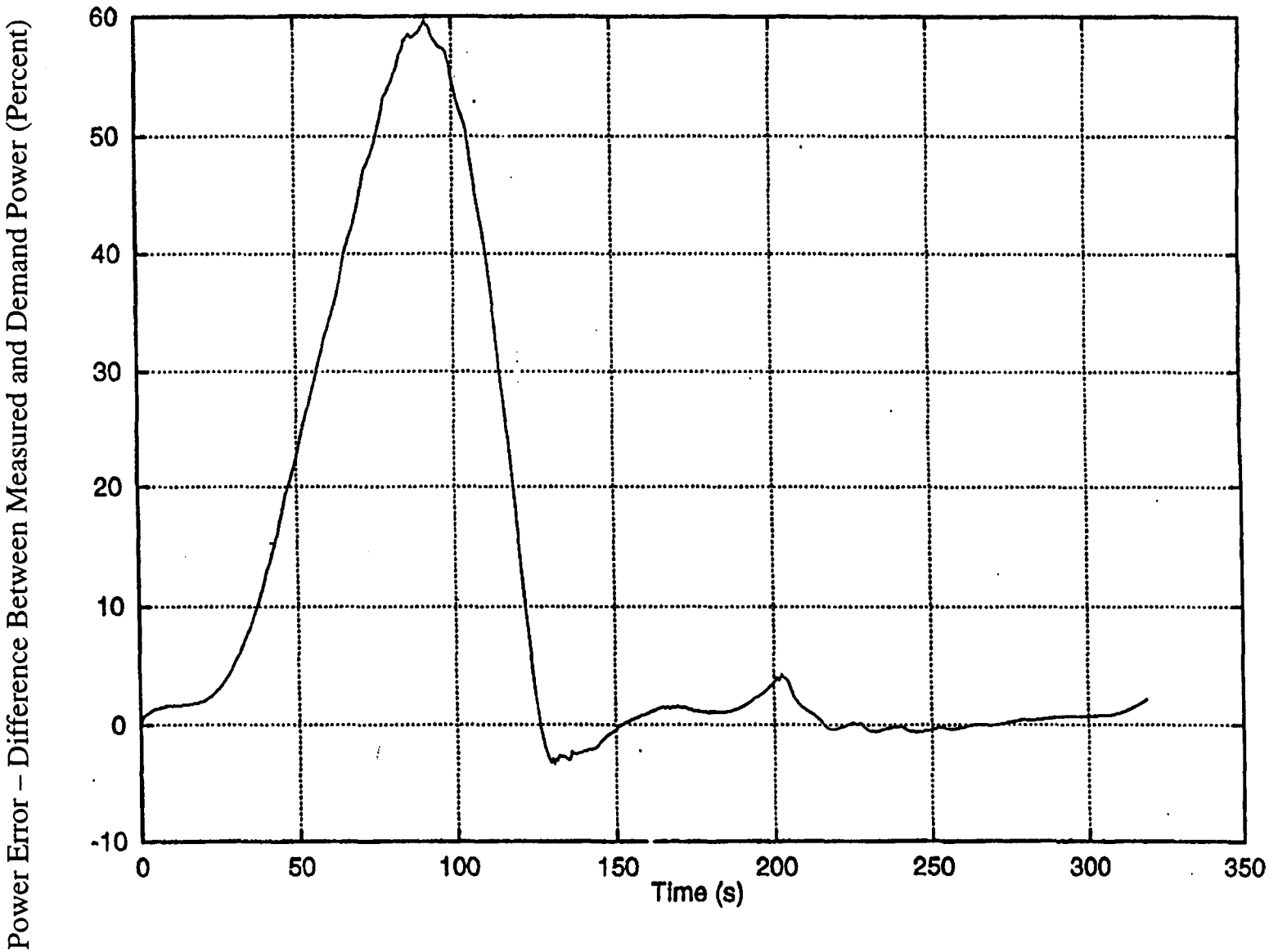

Figure 8.3 In-Core-LOCA Test – Power Transient (CERBRRS Results)

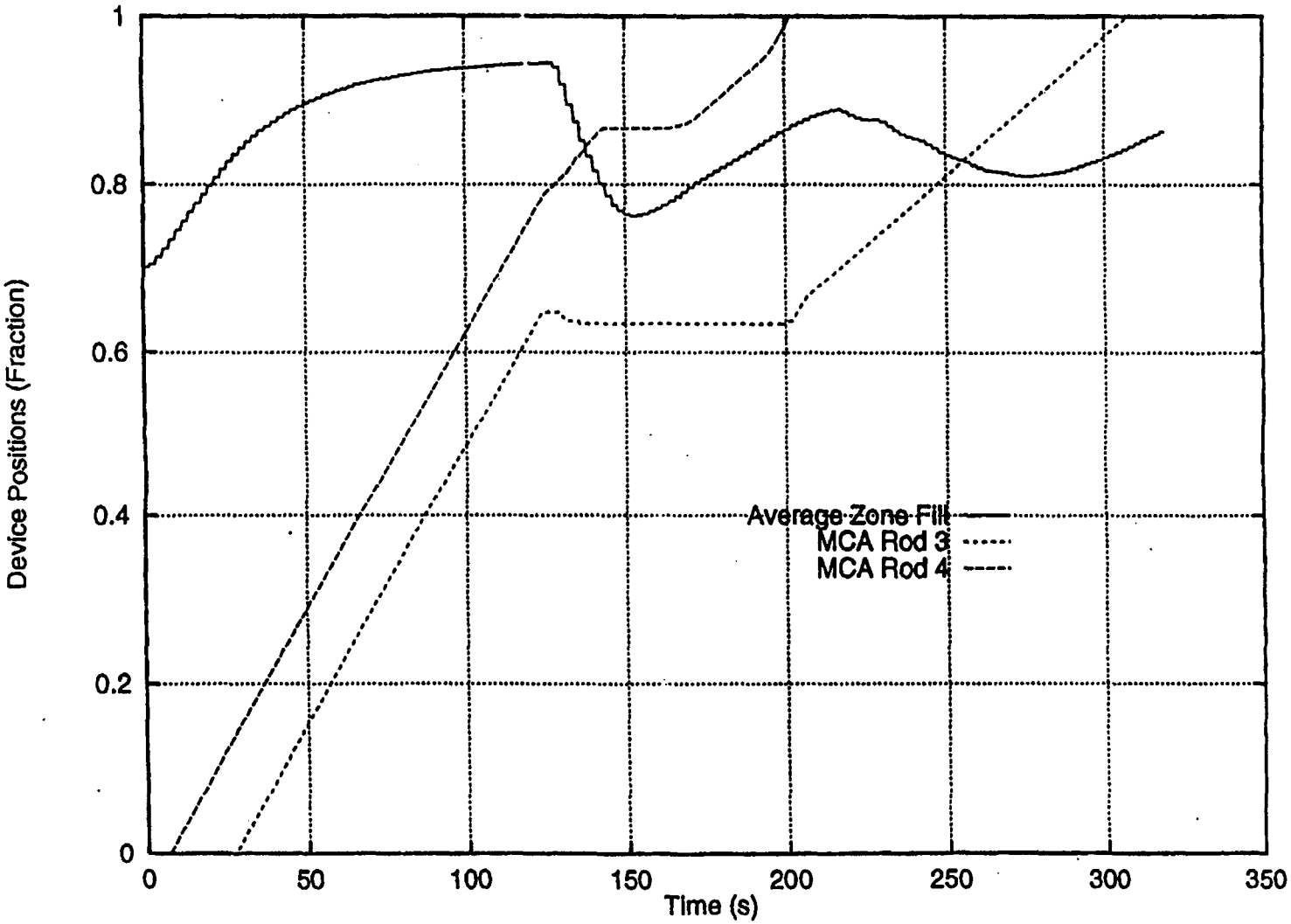

Figure 8.4 In-Core-LOCA Test – Average Zone Fills, Device Pos. (CERBRRS Results)